NUMERICAL SOLUTIONS FOR A CLASS OF SINGULAR NEUTRAL FUNCTIONAL DIFFERENTIAL EQUATIONS

by

Pedro Perez-Nagera

APPROVED BY SUPERVISORY COMMITTEE:

Janos Turi, Chair

Qingwen Hu

Viswanath Ramakrishna

Dmitrii Rachinskii

Dedicated to my family.

NUMERICAL SOLUTIONS FOR A CLASS OF SINGULAR NEUTRAL FUNCTIONAL DIFFERENTIAL EQUATIONS

by

PEDRO PEREZ-NAGERA, BS

DISSERTATION

Presented to the Faculty of

The University of Texas at Dallas

in Partial Fulfillment

of the Requirements

for the Degree of

DOCTOR OF PHILOSOPHY IN

MATHEMATICS

THE UNIVERSITY OF TEXAS AT DALLAS

December 2017

ACKNOWLEDGMENTS

I would like to take this opportunity to show my gratitude to my advisor Dr. Janos Turi for his guidance and expertise. His encouragement and patience throughout this endevour made the completion of this work possible. I would also like to thank my committee members, Drs. Qingwen Hu, Viswanath Ramakrishna, and Dmitrii Rachinskii, for reviewing this work.

I would like to express my gratitude to my family for their continuous support and encouragement throughout my studies.

I am also very grateful to all the professors and teachers who have had a positive impact on my academic career.

August 2017

NUMERICAL SOLUTIONS FOR A CLASS OF SINGULAR NEUTRAL FUNCTIONAL DIFFERENTIAL EQUATIONS

Pedro Perez-Nagera, PhD
The University of Texas at Dallas, 2017

Supervising Professor: Janos Turi, Chair

In this dissertation we study numerical solutions for certain classes of singular neutral functional differential equations (SNFDEs). We begin with an approximation scheme based on piecewise linear approximating spline functions which is used to find numerical solutions for a class of scalar singular neutral equations. The weakly singular kernel that appears in the equation leads to a degradation in the numerical rate of convergence of the approximate solution to the true solution. By modifying the scheme using a graded mesh adapted to the kernel the rate of convergence is restored. Numerical examples and a supporting lemma on the discretization error provide evidence that this is achieved. The approximation scheme is then extended to a SNFDE system. We show that the scheme is convergent provided the mesh is uniform and that there is sufficient smoothness in the true solution. The particular system considered here is a simplified version of an SNFDE that describes the dynamics of a two-dimensional thin airfoil in uniform flow. We provide a numerical example and discuss numerical difficulties. As an application of the approximation scheme we construct a simple forcing function to stabilize the SNFDE.

TABLE OF CONTENTS

LIST OF FIGURES

LIST OF TABLES

CHAPTER 1

INTRODUCTION

A retarded functional differential equation (RFDE) is a differential equation in which the derivative of the current state can depend on its past values as well. In various realistic models describing natural phenomena the derivative of the current state also depends on past values of its derivative. Such equations are known as neutral functional differential equations (NFDE). NFDEs arise naturally in various disciplines including biology, economics, and engineering, see for example [10]. As an example, we can consider the scalar equation

$$\frac{d}{dt}[x(t) - a_1 x(t-1)] = a_2 x(t) + a_3 x(t-1) + f(t),$$

$t \geq 0$, where a_1, a_2, and a_3 are given constants, $f(t)$ is a given function, and $x(t)$ is the unknown function. From this example it is clear that RFDEs and ordinary differential equations are special cases of neutral functional differential equations. Additionally, as in the retarded case, it is clear that the initial data required to advance the solution is a function defined on the interval $[-1, 0]$. An extensive study of a broad class of retarded and neutral functional differential equations was done by Hale and Lunel in [14]. A less understood class of equations are those known as singular NFDEs (SNFDEs). A typical SNFDE is an equation in which $x(t)$ does not appear explicitly on the left hand side of the equation. As an example, we can consider the scalar SNFDE

$$\frac{d}{dt}\left(\int_{-1}^{0} |\theta|^{-1/2} x(t+\theta)\, d\theta\right) = f(t),$$

$t \geq 0$, $f(t)$ is a given function, and $x(t)$ is the unknown function. We can again observe that we need an initial function defined on the interval $[-1, 0]$ to advance the solution. Additionally, from the form of the equation we can observe that there exists a connection between certain SNFDEs and integral equations with a weakly singular kernel.

Numerical approximation methods for NFDEs are well developed and typically they are extensions from numerical approximation methods for RFDEs (compare [2] and [21]). In this dissertation we will study approximate solutions and their convergence properties to SNFDEs.

1.1 Statement of Problem

For certain scalar SNFDEs it was observed in [19] that the rate of convergence of the approximate solution to the true solution was less than the expected second-order convergence. Furthermore, it was conjectured to be directly related to the strength of the singularity in the kernel. We want to restore this degraded rate of convergence to the expected rate of convergence by employing a mesh that is adapted to the particular SNFDE being considered.

We will consider approximation schemes for certain SNFDEs which contain a neutral component coupled with a singular neutral component. The form of this equation is motivated by an application that appears in certain aeroelastic systems described in [5]. We want to establish convergence of the approximation scheme. Lastly, we want to present a preliminary numerical study on the stabilization of the associated finite-dimensional system.

1.2 Contribution

By employing a graded mesh (as an alternative to the uniform mesh) that arises naturally from the SNFDE itself we restore the expected rate of convergence. We provide numerical examples and a supporting lemma on the minimality of the discretization error. To conclude, we explore the flexibility of the approximation scheme by applying it to equations of neutral type.

We consider approximate solutions for the SNFDE system mentioned above and we prove directly the convergence of an approximation scheme previously discussed in [16].

We also present a preliminary numerical study on the stabilization of the associated finite-dimensional system. As an application of the approximation scheme we construct a simple forcing function to stabilize the SNFDE.

1.3 Outline

This dissertation is organized as follows. In Chapter 2 we provide an introduction to neutral and singular neutral functional differential equations. We introduce atomic, non-atomic, and weakly atomic difference operators and discuss their connection to well-posedness. We also discuss the stabilizability and approximation of certain neutral differential equations. In Chapter 3 we consider an approximation scheme for a class of scalar singular neutral differential equations. We introduce graded meshes as a substitute for the uniform mesh with the goal of restoring the lost rate of convergence. We provide numerical case studies to observe the dependence of the rate of convergence on the kernel and we give a supporting lemma. In Chapter 4 we extend the approximation scheme to the singular neutral system case. We discuss the convergence and we give a preliminary numerical study of this system concerning the stabilization of the discretized system. We also discuss numerical difficulties and provide sample Matlab code used in the computation of solutions. In Chapter 5 we provide a summary of this dissertation and discuss possible future work.

1.4 Notation

We now introduce the notation to be used in the following chapter. The space of continuous $\mathbb{R}^n$-valued functions defined on the interval $[a,b]$ will be denoted by $C([a,b];\mathbb{R}^n)$. $L^2([a,b];\mathbb{R}^n)$ will denote the Lebesgue space of $\mathbb{R}^n$-valued (classes of) functions defined on $[a,b]$ whose components are square-integrable. $W^{1,2}([a,b];\mathbb{R}^n)$ denotes the space of $\mathbb{R}^n$-valued absolutely continuous functions which have a derivative in $L^2([a,b];\mathbb{R}^n)$. For the case when $a=-r$ and $b=0$, then we will simply write $C := C([-r,0];\mathbb{R}^n)$, $L^2 := L^2([-r,0];\mathbb{R}^n)$, and $W^{1,2} := W^{1,2}([a,b];\mathbb{R}^n)$. The weighted L^2 space with weight function g is denoted by $L^2_g = L^2_g([a,b];\mathbb{R}^n)$. Letting $r > 0$ the function $x_t : [-r, 0] \longrightarrow \mathbb{R}^n$, for $0 \leq t < \infty$, will be defined by $x_t(s) := x(t+s)$, $-r \leq s < 0$.

CHAPTER 2

PRELIMINARIES

In this chapter we introduce the notion of neutral and singular neutral functional differential equations. We discuss atomic and weakly atomic operators and discuss their relationship to well-posedness. Namely, we discuss that a sufficient condition for well-posedness of certain neutral differential equations is that the difference operator be atomic at zero. In the case of certain singular neutral differential equations, we will discuss that a necessary condition for well-posedness is that the difference operator be weakly atomic. In [5] an aeroelastic system was derived which describes the motion of a two-dimensional airfoil in uniform flow. This system was given in the form of a singular neutral equation and thus it is a motivating application for this study. We conclude this chapter with a discussion on previous approximation methods for neutral differential equations.

2.1 Neutral Functional Differential Equations

In this section we introduce the concept of a neutral functional differential equation and give a summary of known existence and uniqueness results.

A typical problem can be stated as follows: find a function $x : [-r, \infty] \longrightarrow \mathbb{R}^n$ such that

$$\frac{d}{dt}Dx_t = Lx_t + f(t), t \geq 0, \tag{2.1.1}$$

$$x_0(s) = \rho(s), -r \leq s \leq 0, \tag{2.1.2}$$

where ρ is a function and the maps L and D are $\mathbb{R}^n$-valued bounded linear operators. Equation (2.1.1) is called a neutral functional differential equation (NFDE) and the operator D is called the difference operator. This operator plays an important role in the well-posedness, stability, and state feedback control of a problem. By a solution here we mean a continuous function x such that Dx_t is continuously differentiable for $t > 0$ with a continuous right-hand derivative at $t = 0$, and (2.1.1)–(2.1.2) are satisfied. A problem is said to be well-posed if there exists a unique solution to the problem that depends on the initial data in a continuous way. From an approximation perspective it is important for the problem to be well-posed. This is because, for ill-posed problems, small changes in the initial data may result in innacurate or unstable numerical solutions. By state space selection we mean the choice of state space where the initial function belongs to. In the case of NFDEs the usual state spaces considered are C and the product space $Z := \mathbb{R}^n \times L^2$. Typically, well-posedness depends on the state space that is being considered.

Consider the case where D and L are restricted to C, i.e., $D, L : C \longrightarrow \mathbb{R}^n$ and $\rho \in C$. By extending the Reisz representation theorem for linear functionals to the vector case we have that there exists a $n \times n$ matrix-valued function η whose entries are of bounded variation on $[-r, 0]$ such that

$$L\varphi = \int_{-r}^{0} d\eta(s)\varphi(s) \tag{2.1.3}$$

where η is a function of bounded variation. Similarly for D, there exists a $n \times n$ matrix-valued function u whose entries are of bounded variation on $[-r, 0]$ such that

$$D\varphi = \int_{-r}^{0} du(s)\varphi(s) \tag{2.1.4}$$

where $\varphi \in C$. Thus we have general representations of D and L in the form of a Riemann-Stieltjes integrals where $d\eta(\cdot)$ and $du(\cdot)$ are $n \times n$ matrices and $\varphi(\cdot)$ a vector-valued function (hence the switched notation inside the integral). We will assume that $u(s) = u(-r) = 0$ for $s \leq -r$, $u(s) = u(0)$ for $s \geq 0$ and that u is right-continuous on $(-r, 0)$. The operator D is said to be atomic at $s = 0$ if the jump $u(0) - u(0^-)$ is non-singular. In the case that D is atomic at $s = 0$ we note that D can be written as

$$D\varphi = H\varphi(0) + \int_{-r}^{0} d\mu(s)\varphi(s) \tag{2.1.5}$$

for $\varphi \in C$ where $H := u(0) - u(0^-)$ and μ is a function of bounded variation on $[-r, 0]$ such that

$$\lim_{\varepsilon \to 0} \operatorname{Var}_{[-\varepsilon,0]}(\mu) = 0. \tag{2.1.6}$$

We note that in (2.1.5), if μ is constant, $D\varphi = H\varphi(0)$ and so equation (2.1.1) becomes an RFDE. On the other hand, if $H \equiv 0$, then the equation becomes an advanced functional differential equation. In the atomic case, without loss of generality we can assume that H is the $n \times n$ identity matrix since it is nonsingular. If the difference operator D is not atomic, it is said to be non-atomic. If L and D have the representations (2.1.3) and (2.1.5), respectively, it was shown in [14] that the problem (2.1.1)–(2.1.2) is a well-posed problem. In some applications, it may be more beneficial to use the product space Z. Let L and D have the same representations. Assume we have initial data $Dx_0 = \eta$ and $x_0 = \varphi$ for $(\eta, \varphi) \in Z$ and $\varphi \in W^{1,2}$. In this case, a solution is a function $x_t \in W^{1,2}$ such that Dx_t is continuously differentiable, and x satisfies the NFDE (2.1.1)–(2.1.2). It was shown in [6] that atomicity of the D operator is a sufficient condition for well-posedness of the NFDE on product spaces of the type Z. For NFDEs with atomic difference operator, the theory is well-developed. See [14] for an extensive general treatment of NFDEs.

In [21], the special case when D and L have the representations

$$D\psi = \psi(0) - \sum_{j=1}^{m} B_j \psi(-r_j) - \int_{-r}^{0} B(s)\psi(s)ds, \tag{2.1.7}$$

and

$$L\psi = \sum_{j=1}^{m} A_j \psi(-r_j) + \int_{-r}^{0} A(s)\psi(s)ds, \tag{2.1.8}$$

was studied. Here, $0 = r_0 < r_1 < \cdots < r_m = r$ and $A(\cdot)$, $B(\cdot)$ are in $L^2([-r, 0]; \mathbb{R}^{n\times n})$, i.e., $A(\cdot)$ and $B(\cdot)$ are matrix functions with square-integrable components. Note that D is atomic at zero. The following coupled initial value integral problem was considered:

$$\begin{aligned} y(t) &= \eta + \int_0^t Lx_s ds + g(t), \\ Dx_t &= y(t), \end{aligned} \tag{2.1.9}$$

for almost all $t \geq 0$, $g \in L^2_{loc}(0, \infty; \mathbb{R}^n)$, with initial data $x_0 = \rho \in L^2$ and $\eta \in \mathbb{R}^n$. It was shown that this problem has a unique pair of solutions $x(t) = x(t; \eta, \rho, g)$ defined on $[-r, \infty)$ and $y(t) = y(t; \eta, \rho, g)$ defined on $[0, \infty)$ and that $x(t)$ and $y(t)$ depend continuously on the initial data η, ρ, and g, i.e., the map

$$(\eta, \rho, g) \mapsto (y(\cdot; \eta, \rho, g), x(\cdot; \eta, \rho, g))$$

is a continuous map from

$$\mathbb{R}^n \times L^2 \times L^2(0, t_1; \mathbb{R}^n) \longrightarrow L^2(0, t_1; \mathbb{R}^n) \times L^2(-r, t_1; \mathbb{R}^n)$$

for any $t_1 > 0$. The existence and uniqueness of solutions largely depends on the regularity and consistency of the initial data given. We will say that the initial data η and ρ are consistent if $D\rho = \eta$. From a practical perspective, D and L are sufficiently general to encompass many applications. For this reason, it is worthy to summarize the following results on existence and uniqueness (see [14] and [21]).

Let D and L have the representations (2.1.7) and (2.1.8), respectively.

Proposition 2.1.1. (see [21])

1.) If g is a continuous function for $t \geq 0$ and $\varphi \in C$, $\eta = D\rho - g(0)$, then $y(t) = y(t; \eta, \rho, g)$, $x(t) = x(t; \eta, \rho, g)$ are continuous on $t \geq 0$ and $t \geq -r$, respectively, $y(t) = Dx_t$ for all $t \geq 0$ and $Dx_t - g(t)$ is continuously differentiable on $t \geq 0$ with

$$\frac{d}{dt}(Dx_t - g(t)) = Lx_t, \quad t \geq 0,$$

$$x_0 = \rho, \quad \rho \in C.$$

2.) If $g(t) = \int_0^t f(s)ds$, $t \geq 0$, with $f \in L^2_{loc}(0, \infty; \mathbb{R}^n)$, and ρ in C, $\eta = D\rho$, then $x(t)$ is continuous for $t \geq -r$, $y(t) = Dx_t \in W^{1,2}_{loc}(0, \infty; \mathbb{R}^n)$ and

$$\frac{d}{dt}Dx_t = Lx_t + f(t)$$

a.e. for $t \geq 0$, with

$$x_0 = \rho, \quad \rho \in C.$$

3.) If g is as in 2 (above) and $\rho \in W^{1,2}$, $\eta = D\rho$, then $y(t) = Dx_t \in W^{1,2}_{loc}(0, \infty; \mathbb{R}^n)$, $x \in W^{1,2}_{loc}(-r, \infty; \mathbb{R}^n)$, and x is the unique solution of

$$\frac{d}{dt} Dx_t = Lx_t + f(t)$$

a.e. on $t \geq 0$, with

$$x_0 = \rho, \quad \rho \in W^{1,2}.$$

4.) If $L = 0$ and $\eta = 0$ then x is the unique solution of the non-homogeneous difference equation

$$Dx_t = g(t)$$

a.e. on $t \geq 0$, with

$$x_0 = \rho, \quad \rho \in L^2.$$

Remark 2.1.1. Recall that for RFDEs as the solution is advanced forward it becomes smoother. This can be observed when we utilize the so called "method of steps" to find the solution. More general NFDEs need not have this property. To see this consider the scalar NFDE

$$\frac{d}{dt}[x(t) - x(t-r)] = 0, t \geq 0,$$

with initial data $x(\theta) = \rho(\theta)$, $-r \leq \theta \leq 0$. Using the initial data we have that $x(t) - x(t-r) = \eta$, where $\eta := \rho(0) - \rho(-r)$. By the method of steps we have that $x(t) = \rho(t-r) + \eta$ for $0 \leq t \leq r$, $x(t) = \rho(t-2r) + 2\eta$ for $r \leq t \leq 2r$, and so on. Suppose that ρ is a continuously differentiable function on $[-r, 0]$ and $\dot{\rho}(0) \neq \dot{\rho}(-r)$. We can see that there exists a discontinuity in the derivative of the solution at all points rk, $k = 0, 1, 2, \ldots$, and so the solution $x(t)$ is continuously differentiable for $t \geq 0$ except at these indicated points. Hence, the solution will not be smoother than the initial function. ■

In this section we observed that atomicity of the difference operator at $s = 0$ is a sufficient condition for well-posedness. Equations with a non-atomic difference operator will be referred to as singular NFDEs (SNFDEs). In the next section we discuss the well-posedness of such equations.

2.2 Singular Neutral Functional Differential Equations

In [6] it was established that atomicity in the difference operator was sufficient for the well-posedness of class of NFDEs. In the same paper, the authors also gave an example of an NFDE with a non-atomic D operator that yielded a well-posed problem. We consider this example next.

Let D be the scalar valued operator $D\psi := \int_{-r}^{0} |s|^{-p}\psi(s)ds$, $0 < p < 1$, and consider the scalar SNFDE

$$\frac{d}{dt}Dx_t = 0, t > 0,$$

$$x_0 = \varphi.$$

Integrating both sides of the equation yields the initial value problem

$$\begin{aligned} Dx_t &= \eta, t \geq 0, \\ x_0 &= \varphi. \end{aligned} \tag{2.2.1}$$

If $p > 1 - 1/q$ and $(\eta, \varphi) \in \mathbb{R} \times L^q$ then the initial value problem (2.2.1) has a unique solution $x(\cdot;\varphi)$ defined for almost all t in $[0, \infty)$. In particular, if $\varphi \in C$ and $\eta \in \mathbb{R}$ then we have that the problem has the unique integrable solution (see [6])

$$x(t) = \beta \int_{-1}^{0} \frac{1}{t-s} \left|\frac{t}{s}\right|^{p} \varphi(s)ds + \beta \int_{0}^{t} \frac{(t-s)^{p-1}}{(t-s)+1} \varphi(s-1)ds + \beta[\eta - D\varphi]t^{p-1},$$

where $\beta := \sin(p\pi)/\pi$, for $t \in (0, 1]$. We can see that if $D\varphi = \eta$ then the solution will also be continuous. We note that the problem (2.2.1) can be reformulated as an Abel integral equation (see [17]) from which the above solution representation follows. It is important to notice that in the case of $p = 1/2$ then $q < 1/(1-1/2) = 2$. Thus the problem is not shown to be well-posed in the product space $\mathbb{R} \times L^2$, i.e., in a Hilbert space. This is important since it implies that we do not have the approximation benefits granted by a Hilbert space setting. The case when $p = 1/2$ and $q = 2$ is of particular interest since it would apply to the aerodynamics problem discussed below. To remedy this setback the weighted L^2 space, L^2_g, was suggested in [7]. We say that $f \in L^2_g := L^2_g([-r,0];\mathbb{R}^n)$ if

$$\left(\int_{-r}^{0} g(s)|f(s)|^2 ds\right)^{1/2} < \infty,$$

where g is a weighting function. Using a weighted L^2 space of this type, an approximation scheme was introduced in [19] for a class of SNFDEs of the form

$$\frac{d}{dt}Dx_t = Lx_t + f(t), t > 0,$$

$$x(s) = \varphi(s), -r \leq s < 0,$$

where $D\varphi = \int_{-r}^{0} g(s)\varphi(s)ds$ and $L\varphi = a_0\varphi(0) + \int_{-r}^{0} a(\theta)\varphi(t+\theta)d\theta + a_1\varphi(-r)$. Here a_0 and a_1 are constants and $a(\cdot)$ is an integrable function. The kernel g has the following properties: g is positive, monotonically increasing, and integrable on $[-r, 0)$, with $g(s) \longrightarrow \infty$ as $s \longrightarrow 0^-$. Note that the kernel g is more general than the Abel kernel considered in [6]. The numerical feasibility of using a weighted L^2 space for non-atomic neutral equations was observed in [19] and so a Hilbert space setting was recovered for the SNFDE case. A particular drawback of a weighted space is that the weighting function will change with every equation.

The SNFDE example given in [6] motivated the search for necessary and (weaker) sufficient conditions required for well-posedness. In [22], a partial result to this question is given in the form of a necessary condition on the difference operator. Consider the scalar initial value problem

$$Dx_t = D\varphi, t \geq 0, \tag{2.2.2}$$

$$x_0 = \varphi, \tag{2.2.3}$$

where D is non-atomic at $s = 0$ and $\varphi \in C$. In [22] the authors introduce the notion of a weakly atomic operator and show that this condition is necessary for well-posedness for a general class of scalar SNFDEs.

Assume that $D\psi := \int_{-r}^{0} \psi(s)d\mu(s)$ where μ is a function of bounded variation on $[-r, 0]$ such that $\mu(s) = 0$ for $s \geq 0$, $\mu(s) = \mu(-r)$ for $s \leq -r$, and μ is left-hand continuous on $(-r, 0)$. The operator D is called weakly atomic if

$$\lim_{\lambda \longrightarrow \infty} |\lambda \triangle_0(\lambda)| = \infty$$

(for $\lambda \in \mathbb{R}$), where

$$\triangle_0(\lambda) := \int_{-r}^{0} e^{\lambda s} d\mu(s).$$

The necessary condition can now be stated as follows: if the problem (2.2.2)–(2.2.3) has a unique continuous solution $x(t; \varphi)$ on $[-r, \infty)$ for each $\varphi \in C$ that also depends continuously on φ, then D must be weakly atomic. Note that if D is atomic, i.e., D has the form $D\varphi = \varphi(0) + \int_{-r}^{0} d\mu(s)\varphi(s)$, then it is also weakly atomic. This follows from

$$\triangle_0(\lambda) = 1 + \int_{-r}^{0} e^{\lambda s} d\mu(s)$$

and

$$\lim_{\lambda \longrightarrow \infty} \int_{-r}^{0} e^{\lambda s} d\mu(s) = 0.$$

Consider the special case when the D operator is of Abel type, i.e.,

$$D\varphi := \int_{-r}^{0} g(s)\varphi(s)ds,$$

where g is a generalized Abel kernel and $0 < r < \infty$. We assume that g has the following properties: g is positive, monotonically increasing, and integrable on $[-r, 0)$, with $g(s) \longrightarrow \infty$ as $s \longrightarrow 0^-$. It is helpful to keep in mind the so-called Abel kernel $|s|^{-p}$ on $[-r, 0)$, with $0 < p < 1$, which represents a possible choice for g. In this case we have that

$$\triangle_0(\lambda) = \int_{-r}^{0} e^{\lambda s} g(s) ds,$$

and therefore

$$\triangle_0(\lambda) = \int_{-r}^{0} e^{\lambda s} g(s) ds \geq \int_{-1/\lambda}^{0} e^{\lambda s} g(s) ds \geq g(-1/\lambda) \int_{-1/\lambda}^{0} e^{\lambda s} ds \geq g(-1/\lambda) \frac{1}{\lambda} \left(1 - \frac{1}{e}\right).$$

It follows that $\lambda \triangle_0(\lambda) \longrightarrow \infty$ as $\lambda \longrightarrow \infty$ and so D is weakly atomic.

In [18] an example of an ill-posed problem in the state space C was given. Let g be as above and consider the problem

$$\frac{d}{dt}\left(\int_{-r}^{0} g(\theta) x(t+\theta) d\theta + x(t-r)\right) = 0, t \geq 0,$$

$$x(t) = \rho(t), -r \leq t \leq 0.$$

The difference operator here is $D\psi = \psi(-r) + \int_{-r}^{0} g(\theta)\psi(\theta) d\theta$ and note that it is atomic at $\theta = -r$. Letting

$$\triangle_1(\lambda) = e^{-\lambda r} + \int_{-r}^{0} e^{\lambda \theta} g(\theta) d\theta, \lambda \in \mathbb{C},$$

the authors were able to show that there exists a sequence of real-valued roots $\lambda_k, k = 1, 2, \ldots,$ for $\triangle_1(\lambda)$ such that $\lim_{k \longrightarrow \infty} \lambda_k = \infty$ implying ill-posedness.

In this section we discussed weakly atomic difference operators and the role they play in well-posedness. In next section we discuss an application that motivated the study of SNFDEs in this dissertation.

2.3 A Motivating Application

In this section we give a brief description of the aeroelastic system that motivates this study (see also [5]). Consider the system

$$\frac{d}{dt}\left(A_0 x(t) + \int_{-r}^{0} A_1(s) x(t+s) ds\right) = B_0 x(t) + \int_{-r}^{0} B_1(s) x(t+s) ds + Gu(t), \qquad (2.3.1)$$

$0 < r \leq \infty$, where A_0 and B_0 are 8×8 matrices and $A_1(s)$ and $B_1(s)$ are 8×8 integrable matrix functions. This system describes the dynamics of a two-dimensional airfoil in incompressible flow. From a practical perspective, this airfoil can be interpreted as a cross-section of a wing of an aircraft. Here, $x(t) \in \mathbb{R}^8$ is given by

$$x(t) := \left(z(t)^T, z'(t)^T, \Gamma(t), \Gamma'(t)\right)^T,$$

where $z(t) := (h(t), \theta(t), \beta(t))$, $h(t)$ is the plunge, $\theta(t)$ is the pitch angle, $\beta(t)$ is the trailing flap angle, $\Gamma(t)$ is the airfoil circulation function, and $u(t)$ is a possible control for a trailing flap. What makes this system interesting is that the last row of the system is an equation of the form

$$\int_{-r}^{0} A_{1_{88}}(s) x_8'(t+s) ds = B_8 x(t)$$

where $A_{1_{88}}(s) = ((Us-2)/Us)^{1/2}$, $-\infty < s < 0$, and U is a constant. Studies of this system have been primarily focused on the finite-delay version, i.e., $0 < r < \infty$. From a control perspective, the initial data could represent small disturbances in the system and we would like to bring the system back to the origin. More explicitly, we are concerned with the stabilizability of the system. In the aeroelastic system (2.3.1) one would like to apply an appropriate control $u(t)$ to the trailing flap to bring the system to rest after vibrations begin. This is commonly referred to as a flutter suppression problem.

In the following section we consider a system of equations that is composed of an NFDE coupled with an SNFDE. For computational simplicity we will consider a simpler system that retains the "partial atomicity".

2.4 A Partially Atomic System

Consider the following equation on the weighted product space $\mathbb{R} \times L_g^2(-r, 0)$ with kernel g:

$$\frac{d}{dt}\left(x(t) + \int_{-r}^{0} a_{12}(s) y_t(s) ds\right) = b_{11} x(t) + b_{12} y_t(0) + \int_{-r}^{0} b_{12}(s) y_t(s) ds + f(t)$$

$$\frac{d}{dt}\left(\int_{-r}^{0} g(s)y_t(s)ds\right) = b_{21}x(t)$$

with initial data

$$x(0) = \eta, \quad y_0 = \varphi,$$

where $y_t(s) := y(t+s)$ for $s \in [-r, 0]$ and $t \geq 0$. This is a 2×2 system where $a_{12}(s)$ and $b_{12}(s)$ are integrable functions and b_{11} and b_{12} are scalars. Furthermore, we will assume that the function g in the second equation satisfies the following conditions: g is positive, monotonically increasing, integrable on $[-r, 0]$, with $g(s) \longrightarrow \infty$ as $s \longrightarrow 0^-$. As before, it is helpful to keep in mind the so-called Abel kernel $|s|^{-p}$ on $[-r, 0)$ with $0 < p < 1$. The right-hand side function, f, is an integrable function that may be thought of as a control. If in the above system we make the following definitions:

$$D_1(\eta, \varphi) := I\eta + \int_{-r}^{0} a_{12}(s)\varphi(s)ds,$$

$$L_1(\eta, \varphi) := b_{11}\eta + b_{12}\varphi(0) + \int_{-r}^{0} b_{12}(s)\varphi(s)ds,$$

$$D_2\varphi := \int_{-r}^{0} g(s)\varphi(s)ds, \text{ and } L_2\varphi := b_{21}\eta,$$

we can now rewrite the above problem as

$$\frac{d}{dt}D_1(x(t), y_t) = L_1(x(t), y_t) + f(t) \tag{2.4.1}$$

$$\frac{d}{dt}D_2 y_t = L_2 x(t) \tag{2.4.2}$$

$$x(0) = \eta, \quad y_0 = \varphi \tag{2.4.3}$$

with $\eta \in \mathbb{R}$ and $\varphi \in C([-r, 0]; \mathbb{R})$.

Note that although the coupled system (2.4.1)-(2.4.2) is simpler than (2.3.1), the interesting relationship where one equation is atomic and the other equation is non-atomic, i.e., singular, still remains. The well-posedness of the system for the particular choice of kernel

$\tilde{g}(s) = (1 - 1/s)^{1/2}$, $-r \le s < 0$, was established in [16] in the state space $\mathbb{R}^7 \times L^2_{\tilde{g}}(-r, 0)$. The result can be restricted to the scalar case considered here, i.e., $\mathbb{R} \times L^2_{\tilde{g}}(-r, 0)$. We note that well-posedness of an infinite-delay version of the SNFDE above was established in [15] on the state space $\mathbb{R}^7 \times L^2_k(-\infty, 0)$, where $k(s) = e^{ws}(1 - 2/(Us))^{1/2}$, $-\infty < s < 0$, U is a positive constant, and $w > 0$ is chosen in a particular way.

2.5 Approximate solutions for NFDEs

Methods for solving NFDEs numerically typically involve approximating the original problem by a sequence of finite-dimensional ordinary differential equations. The fact that we are approximating an infinite-dimensional problem by a finite-dimensional problem is important for computational purposes. A satisfactory method is one which produces a numerical solution that converges to the solution of the original problem as we increase the dimension of the approximating subspace. We recall the following scheme to introduce the reader to the commonly used method of "averaging projections" and to put the approximation scheme in the following chapters in perspective. The averaging projection method has been used for RFDEs and NFDEs, see for example, [1] and [21], respectively. We provide [21] and [36] as references for a more general treatment of the following scheme.

Consider the scalar NFDE

$$\frac{d}{dt} D x_t = L x_t + f(t), t \ge 0,$$

$$x_0 = \rho, \rho \in C,$$

where $r > 0$, f is a locally integrable function, and the operators D and L are defined by

$$D\varphi := \varphi(0) + A\varphi(-r) \quad \text{and} \quad L\varphi := B\varphi(0) + C\varphi(-r).$$

The NFDE is first reformulated into an abstract Cauchy problem. To this end we define $z(t) = (Dx_t, x_t)$ and the operator $\mathcal{A}$ by

$$\mathcal{D}(\mathcal{A}) := \{(\eta, \varphi) \in Z = \mathbb{R} \times L^2 : \varphi \in W^{1,2}, \eta = \varphi(0) + A\varphi(-r)\},$$

$$\mathcal{A}(\eta, \varphi) := (L\varphi, \dot{\varphi}) = (B\varphi(0) + C\varphi(-r), \dot{\varphi}).$$

By direct computation we can see that

$$\frac{d}{dt}z(t) = \mathcal{A}z(t) + (f(t), 0),$$

$$z(0) = (\eta, \rho),$$

for $(\eta, \varphi) \in \mathcal{D}(\mathcal{A})$. Once the problem is reformulated we can construct a sequence of approximating ordinary differential equations that yield a sequence of approximating solutions that will converge to $z(t)$. We now define the approximation scheme.

Let $Z := \mathbb{R} \times L^2$, N be a positive integer, and define $\tau_j^N = -j\frac{r}{N}$, $j = 0, 1, 2, \ldots N$, i.e., the interval $[-r, 0]$ is partitioned into N subintervals. This partition is used to define the subspace $Z^N \subset Z$ by

$$Z^N := \{(\eta, \varphi) \in Z : \varphi = \sum_{j=1}^{N} \varphi_j^N \chi_j^N, \varphi_j^N \in \mathbb{R}^n\},$$

where χ_j^N is the characteristic function on $[\tau_j^N, t_{j-1}^N)$. Define the orthogonal projection $P^N : Z \longrightarrow Z^N$ by

$$P^N(\eta, \rho) = (\eta, \rho^N),$$

where

$$\rho^N = \sum_{j=1}^{N} \rho_j^N \chi_j^N, \quad \text{and} \quad \rho_j^N = \frac{1}{\tau_{j-1} - \tau_j} \int_{\tau_j^N}^{\tau_{j-1}^N} \rho(\theta) d\theta.$$

By the domain condition of $\mathcal{A}$ we have that $\eta = D\rho = B\rho(0) + C\rho(-r)$. Substituting ρ^N into this equation we get $\rho_0^N = \eta - A\rho_N^N$. Thus, we define the approximating operator $\mathcal{A}^N : Z \longrightarrow Z^N$ by

$$\mathcal{A}^N(\eta, \rho) = \mathcal{A}^N P^N(\eta, \rho) = (B\rho_0^N + C\rho_N^N, \sum_{j=1}^{N} \psi_j^N \chi_j^N),$$

where

$$\psi_j^N = \frac{N}{r}(\rho_{j-1}^N - \rho_j^N), j = 1, 2, \ldots, N.$$

Together, the set Z^N, P^N, and $\mathcal{A}^N$ is referred to as the averaging projections approximation scheme. Spline approximations have also been studied exensively for RFDEs and NFDEs in [1] and [2], respectively. This approximation scheme induces a sequence of $N+1$-dimensional differential equations of the form

$$\frac{d}{dt}z^N(t) = \mathcal{A}^N z^N(t) + P^N(f(t), 0), t \geq 0,$$

$$z^N(0) = P^N(\eta, \rho) \in Z^N.$$

Under certain conditions (dissipativity and density) on the sequence of operators $\mathcal{A}^N$, one can argue that the sequence of solutions for the finite-dimensional problems, $z^N(t)$ for $N = 1, 2, \ldots$, converges to the solution of the orignal problem, $z(t)$, i.e., $z^N(t) \longrightarrow z(t)$ as $N \longrightarrow \infty$. A detailed explanation of these conditions requires introducing the concept of linear operator semigroups, which is peripheral to this dissertation. Hence, we will only refer the interested reader to the references [2], [21], and [31]. From a computational perspective, we need to define a basis for Z^N. For example, since Z^N is a Euclidean space, we can define the basis $e_0^N := (1, \sigma)$ and $e_j^N := (0, \chi_j^N)$, $j = 1, 2, \ldots, N$, where σ is the zero function. Let $w_j^N(t)$ be time dependent coefficients such that $\sum_{j=0}^N w_j^N(t) e_j^N = z^N(t)$. The reader will notice that this a step function representation of $z^N(t)$. Substituting this representation into the approximating system, we arrive at

$$\dot{w}_0^N(t) = B(w_0^N(t) - Aw_N^N(t)) + Cw_N^N(t) + f(t)$$

with

$$\dot{w}_j^N(t) = \frac{N}{r}(w_{j-1}^N(t) - w_j^N(t)),$$

$j = 1, 2, \ldots, N$. We can see that this is equivalent to an ordinary differential equation system of the form $\dot{w}^N(t) = A^N w^N(t) + F^N(t)$, where $w^N(t) = (w_0^N(t), w_1^N(t), \ldots, w_N^N(t))^N$, A^N is an appropriate $(N+1)\times(N+1)$ matrix (see [21]), and $F^N(t) = (f(t), 0, \ldots, 0)^N$. The initial data is provided by

$$w^N(0) = (\eta, \rho_1^N, \rho_2^N, \ldots, \rho_N^N)^T.$$

In the case of RFDEs, it is under this formulation that an optimal control framework has been well developed, see for instance [1]. This is important in applications where one needs to stabilize a system, e.g., the aeroelastic system presented above. The forthcoming numerical scheme for SNFDEs is similar in spirit, however, for SNFDEs a weighted L^2 space was considered in place of a product space. To the author's knowledge, an optimal control formulation for SNFDEs is yet to be developed.

We now turn our attention to constructing a numerical scheme for scalar SNFDEs and we discuss the numerical issues induced by the weakly atomic difference operator.

CHAPTER 3

APPROXIMATIONS FOR SCALAR SINGULAR NEUTRAL FUNCTIONAL DIFFERENTIAL EQUATIONS

In this chapter we present case studies to illustrate the dependence of the rate of convergence of numerical schemes for singular neutral equations (SNFDEs) on the particular mesh employed in the computation. The numerical experiments in [19] demonstrated a "degradation" of the expected rate of convergence when uniform meshes were considered. In particular, it was observed numerically that the degradation of the rate of convergence was related to the strength of the singularity in the kernel of the SNFDE. Following the idea used for Volterra equations with weakly singular kernels (see e.g., [3] and [4]) we investigate graded meshes associated with the kernel of the SNFDE in attempting to restore convergence rates. We give an estimate for the global rate of convergence for on a fixed time interval. Finally, to illustrate the flexibility of the scheme presented we present numerical examples of the scheme applied to equations that are not of singular type.

3.1 Introduction

Consider the following SNFDE in the state space $L^2_g(-r,0)$, a weighted L^2-space with kernel g:

$$\frac{d}{dt}\left(\int_{-r}^{0} g(\theta)x(t+\theta)d\theta\right) = f(t),\ t>0,\ 0<r<\infty, \tag{3.1.1}$$

with initial condition

$$x(\theta)=\rho(\theta) \text{ for } -r\le\theta<0 \tag{3.1.2}$$

where ρ is in $L^2_g(-r,0)$. The kernel g appearing in (3.1.1) is positive and nondecreasing on $(-r,0)$ and weakly singular at zero. More precisely, $g(s)>0$ and $g'(s)\ge 0$ on $(-r,0)$ with $g(s)\to\infty$ as $s\to 0^-$ but still integrable, i.e., $g\in L^1(-r,0)$. The right-hand side function , f, is an integrable function. We note that an equation of this type occurs in certain aeroelastic systems (see [5]). Using the notation for neutral functional differential equations (NFDE), (3.1.1) could be rewritten as

$$\frac{d}{dt}Dx_t = f(t), \tag{3.1.3}$$

where the difference operator D is the bounded linear operator $D\varphi := \int_{-r}^{0} g(s)\varphi(s)ds$ and recall that x_t is the solution segment, i.e., $x_t(\theta) = x(t+\theta)$, $\theta \in [-r, 0]$. It was shown in [7, 19] that (3.1.1)–(3.1.2) is well-posed on a weighted L^2-space.

This chapter is organized as follows. In Section 3.2 we introduce finite dimensional approximations for the SNFDE (3.1.1)–(3.1.2). We also discuss graded discretizations of the interval $[-r, 0]$ in the construction of numerical schemes. In Section 3.3 we explore the degradation of the convergence rate in the scheme discussed in Section 3.2. In Section 3.4 we present case studies to illustrate the dependence of the numerically observed rate of convergence on mesh selection. We make concluding remarks in Section 3.5.

3.2 Numerical Approximations

To construct numerical schemes, we proceed as in [19] and convert the SNFDE (3.1.1)-(3.1.2) into a first order hyperbolic partial differential equation (PDE) with nonlocal boundary conditions. The initial data at $t = 0$ is given by the initial function $\rho(\theta)$, $-r \leq \theta \leq 0$ and the boundary is generated by the neutral equation itself. Define $\varphi(t,\theta) := x(t+\theta)$ for $-r < \theta < 0$ and $t \geq 0$. Assuming that φ is differentiable it satisfies the PDE

$$\frac{\partial}{\partial t}\varphi(t,\theta) = \frac{\partial}{\partial \theta}\varphi(t,\theta), \tag{3.2.1}$$

for $t > 0$, $-r < \theta < 0$. Furthermore, it follows from (3.2.1) that the boundary condition for $t > 0$ can be written as

$$\int_{-r}^{0} g(\theta)\frac{\partial}{\partial \theta}\varphi(t,\theta)d\theta = f(t). \tag{3.2.2}$$

Remark 3.2.1. In the (t, θ)-plane, $\varphi(t, \theta)$ along $(0, \theta)$, $-r \le \theta < 0$, is given by the initial condition $\rho(\theta)$. For $t > 0$, the right boundary, i.e., $\varphi(t, 0)$, can be obtained from (3.2.2) and then $\varphi(t, \theta)$, $t > 0, -r \le \theta < 0$ is determined along the characteristic lines. Using this perspective one may construct other numerical schemes similar to the one presented here. ■

We begin by constructing the approximating function. Let N be a positive integer and introduce the partition of the interval $[-r, 0]$ as $-r =: \tau_N^N < \tau_{N-1}^N < \cdots < \tau_1^N < \tau_0^N := 0$ and let $\delta_j^N := \tau_{j-1}^N - \tau_j^N > 0$ for $1 \le j \le N$. We define

$$\varphi^N(t, \theta) := \sum_{j=0}^{N} \alpha_j^N(t) B_j^N(\theta) \text{ for } t \ge 0, -r \le \theta \le 0,$$

where the piecewise linear functions, B_j^N, $j = 0, 1, 2, ..., N$ are given as

$$B_j^N(\theta) := \begin{cases} (\theta - \tau_{j+1}^N)/\delta_{j+1}^N & \theta \in [\tau_{j+1}^N, \tau_j^N], \\ (\tau_{j-1}^N - \theta)/\delta_j^N & \theta \in [\tau_j^N, \tau_{j-1}^N], \\ 0 & otherwise \end{cases} \text{ for } j = 1, 2, ..., N-1, \tag{3.2.3}$$

$$B_0^N(\theta) := \begin{cases} (\theta - \tau_1^N)/\delta_1^N & \theta \in [\tau_1^N, \tau_0^N], \\ 0 & otherwise \end{cases}, \tag{3.2.4}$$

and

$$B_N^N(\theta) := \begin{cases} (\tau_{N-1}^N - \theta)/\delta_N^N & \theta \in [\tau_N^N, \tau_{N-1}^N], \\ 0 & otherwise \end{cases}, \tag{3.2.5}$$

and $\alpha_j^N(t)$, $j = 0, 1, 2, ..., N$ are time dependent coefficients. One option is to use uniform mesh in space, i.e., to select $\delta_j = \delta = \frac{r}{N}$. A more involved option is to use a graded mesh, that is, select δ_j, $j = 1, 2, ..., N$, specifically for the particular SNFDE under consideration. Graded meshes were applied in a collocation scheme in [4] to solve Volterra integral equations of the second kind with weakly singular kernels and results on attainable optimal rates of convergence were given. In this dissertation SNFDEs with weakly singular kernels are considered including kernels of the type $g(t) = t^{-p}$, with $0 < p < 1$, and thus the results in [4] served as a motivation to introduce graded meshes into the schemes presented here. In particular, we choose the mesh such that the area of the integral of the kernel of the SNFDE is the same on each subinterval, that is, we choose all τ_j^N such that

$$\int_{\tau_j^N}^{\tau_{j-1}^N} g(\theta)d\theta = \frac{1}{N}\int_{-r}^{0} g(\theta)d\theta \tag{3.2.6}$$

for $1 \leq j \leq N$ and where $g(\theta)$ is the kernel in equation (3.1.1). This mesh is applied for most examples in Section 4 (note that in Example 3.4.5 it is somewhat modified to accommodate a more complicated kernel). Throughout our computations we use uniform time steps of size Δt on the interval $[0, T]$, where $T > 0$ denotes the final time. To simplify notation, the superscript N will be omitted during the remainder of this section.

Remark 3.2.2. While uniform meshes yield simpler schemes, especially when the space (δ) and time (Δt) discretization is selected such that $\delta = \Delta t$, their application lead to a degradation of the expected rate of convergence (see e.g., [19] for numerically observed rates of convergence). The numerical findings in [19] indicated that the degradation of the rate of convergence was directly related to the strength of the weak singularity in the kernel of the SNFDE. A dependence on the kernel singularity was also noted in [11], [12] and [26], in the context of numerical solutions of Abel integral equations, namely convergence rates of $2 - p$ were obtained for the kernels t^{-p}, $0 < p < 1$ when using a midpoint method with uniform mesh. Motivated by the analysis in [11] we present in this dissertation rate of convergence estimates for numerical schemes for SNFDEs (see Lemma 3.3.1 below). In particular, we arrive at a discretization error of order $2 - p$ in the uniform mesh case and order 2 in the graded mesh case, respectively, when we consider the difference of the integral in the boundary condition (3.2.2) and its fully discretized analog in equation (3.2.11). The numerical case studies in Section 4 indicate that the graded mesh (3.2.6) is a viable candidate to prevent the "degradation" of the expected convergence rate of 2 for the numerical schemes (3.2.12) for SNFDEs with more general weakly singular kernels as well. ■

Remark 3.2.3. See also [8] and [9] for related results on mesh selection. In [8], an alternative method to solve a similar class of SNFDEs is given where the authors first convert the SNFDE to a Volterra equation of second kind which is then solved using a hybrid collocation method. ■

Assume that a mesh is specified and consider a second-order space discretization to equation (3.2.1) (see [19]):

$$\frac{d}{dt}\left(\frac{\alpha_{j-1}(t)+\alpha_j(t)}{2}\right) = \frac{1}{\delta_j}(\alpha_{j-1}(t)-\alpha_j(t)) \tag{3.2.7}$$

for $1 \leq j \leq N$ and substitute $\varphi^N(t,\theta)$ into the boundary condition (3.2.2) to advance the solution to obtain

$$\sum_{j=1}^{N} \frac{g_j}{\delta_j}(\alpha_{j-1}(t)-\alpha_j(t)) = f(t), \tag{3.2.8}$$

where $g_j := \int_{\tau_j}^{\tau_{j-1}} g(\theta)d\theta$. Equations (3.2.7)-(3.2.8) form the semi-discrete scheme.

Using the second-order implicit trapezoidal rule in time in (3.2.7), we get the fully discretized scheme

$$\frac{1}{\Delta t}\left(\frac{\alpha_{j-1}^{k+1}+\alpha_j^{k+1}}{2} - \frac{\alpha_{j-1}^{k}+\alpha_j^{k}}{2}\right) = \frac{1}{2\delta_j}\left(\alpha_{j-1}^{k+1}-\alpha_j^{k+1}+\alpha_{j-1}^{k}-\alpha_j^{k}\right), \tag{3.2.9}$$

or, equivalently,

$$\alpha_{j-1}^{k+1}C_j + \alpha_j^{k+1} = \alpha_{j-1}^{k} + \alpha_j^{k}C_j, \tag{3.2.10}$$

where $C_j = \left(\frac{1}{\Delta t} - \frac{1}{\delta_j}\right) / \left(\frac{1}{\Delta t} + \frac{1}{\delta_j}\right)$. The right boundary, α_0^{k+1}, is computed from the equation

$$\sum_{j=1}^{N} \frac{g_j}{\delta_j}(\alpha_{j-1}^{k+1}-\alpha_j^{k+1}) = f((k+1)\Delta t). \tag{3.2.11}$$

Since we are considering the second-order discretization (3.2.7) in space and the second-order discretization (3.2.9) in time for equation (3.2.1), it is reasonable to expect second-order convergence to the true solution. We now have a system of linear equations to determine α_j^{k+1}, $j = 0, 1, 2, ..., N$, namely

$$\mathbf{K}_1 \mathbf{a}^{k+1} = \mathbf{K}_2 \mathbf{a}^k + \mathbf{F}^{k+1}, \tag{3.2.12}$$

$k \geq 0$, where

$$\mathbf{K}_1 := \begin{pmatrix} \frac{g_1}{\delta_1} & \left(\frac{g_2}{\delta_2} - \frac{g_1}{\delta_1}\right) & \cdots & \cdots & \left(\frac{g_N}{\delta_N} - \frac{g_{N-1}}{\delta_{N-1}}\right) & -\frac{g_N}{\delta_N} \\ C_1 & 1 & 0 & ... & 0 & 0 \\ 0 & C_2 & 1 & ... & 0 & 0 \\ \vdots & \vdots & \ddots & \ddots & 0 & 0 \\ 0 & 0 & ... & C_{N-1} & 1 & 0 \\ 0 & 0 & ... & 0 & C_N & 1 \end{pmatrix}, \mathbf{a}^k := \begin{pmatrix} \alpha_0^k \\ \alpha_1^k \\ \alpha_2^k \\ \vdots \\ \alpha_{N-1}^k \\ \alpha_N^k \end{pmatrix},$$

$$\mathbf{K}_2 := \begin{pmatrix} 0 & 0 & 0 & \cdots & 0 & 0 \\ 1 & C_1 & 0 & ... & 0 & 0 \\ 0 & 1 & C_2 & ... & 0 & 0 \\ \vdots & \vdots & \ddots & \ddots & 0 & 0 \\ 0 & 0 & ... & 1 & C_{N-1} & 0 \\ 0 & 0 & ... & 0 & 1 & C_N \end{pmatrix}, \text{ and } \mathbf{F}^k := \begin{pmatrix} f((k+1)\Delta t) \\ 0 \\ 0 \\ \vdots \\ 0 \\ 0 \end{pmatrix}.$$

Note that we have placed $\mathbf{F}^{k+1}$ on the right side of the equation since it is assumed to be a known quantity. If the mesh is uniform, i.e., $\delta_j = \delta$, $j = 1, 2, ..., N$ and $\delta = \Delta t$, then $C_j = 0$ for all j and we get the particular scheme with uniform mesh considered in [19].

Remark 3.2.4. Note that the matrix $\mathbf{K}_1$ in (3.2.12) is nonsingular for all N for Abel-type kernels considered in the forthcoming examples. ■

Remark 3.2.5. The convergence of both the semi-discrete (3.2.7)-(3.2.8) and fully-discrete (3.2.10)-(3.2.11) schemes were established in [19]. ■

We now give a few words to explain system (3.2.12). At time $t = 0$ we have that $\alpha_j^0 = \rho(\tau_j)$ for $j = 1, ..., N$ and α_0^0 can be computed from (3.2.11) (with $k = -1$). Thus the vector $(\alpha_0^0, \alpha_1^0, ..., \alpha_{N-1}^0, \alpha_N^0)^T$ is known and will be used to compute $(\alpha_0^1, \alpha_1^1, ..., \alpha_{N-1}^1, \alpha_N^1)^T$. In a similar fashion the vector of unknowns at step $(k+1)\Delta t$, $(\alpha_0^{k+1}, \alpha_1^{k+1}, ..., \alpha_{N-1}^{k+1}, \alpha_N^{k+1})^T$, will be computed using $(\alpha_0^k, \alpha_1^k, ..., \alpha_{N-1}^k, \alpha_N^k)^T$ for all remaining $k \geq 1$. Assume we are interested in approximating the true solution $x(k\Delta t)$ up to time-step k_T. Then, the solution is approximated by $\varphi^N(k\Delta t, 0)$ (since $\theta < 0$ introduces a delay) and so the numerical solution is continuously advanced by the α_0^k component (the right boundary mentioned above) in each newly computed vector up to step k_T. That is, the numerical solution up to time-step k_T is given by the values $\alpha_0^1, \alpha_0^2, ..., \alpha_0^{k_T-1}$, and $\alpha_0^{k_T}$.

In this section we introduced a family of fully-discrete schemes with uniform and graded meshes for the numerical solution of SNFDEs with weakly singular kernels. In the next section we establish error estimates for both cases for a special class of weakly singular kernels.

3.3 On the rate of convergence

Recall that the approximate solution is computed using the nonlocal boundary condition (3.2.2). For this reason, to study the convergence rate of the approximate solution to the true solution, we should understand how fast the fully-discretized version of the integral converges to the true value of the integral in (3.2.2). It is reasonable to expect that the global rate of convergence of the scheme would most likely benefit from a better approximation of the integral in (3.2.2) and therefore we make the characterization of this discretization error the main objective of this section.

At time $t_{k+1} > 0$, we want to establish a local consistency error bound between the integral

$$J := \int_{-r}^{0} g(\theta)\frac{\partial}{\partial\theta}\varphi(t_{k+1},\theta)d\theta$$

and its fully-discretized analog given by

$$K := \sum_{j=1}^{N} \frac{g_j}{\delta_j}(\varphi(t_{k+1},\tau_{j-1}) - \varphi(t_{k+1},\tau_j)),$$

where φ is the true solution of (3.2.1)-(3.2.2). By a local consistency error we mean how well the discretized version of the integral approximates the true integral. Consider a kernel g of the form $g(\theta) = |\theta|^{-p}$, $0 < p < 1$, and assume $\varphi(t_{k+1},\cdot) \in C^3[-r,0]$. The smoothness is assumed to accomodate a Taylor series appoach for the error analysis. First, we establish the following global convergence rate confirming the global rate of convergence with uniform mesh.

We have the following result (see [32]):

Lemma 3.3.1. *Let N be a positive integer, $t_{k+1} > 0$, $g(\theta) = |\theta|^{-p}$, $0 < p < 1$ for $\theta \in [-r,0)$, $r > 0$, and assume that the solution of (3.2.1)-(3.2.2), $\varphi(t_{k+1},\cdot) \in C^3[-r,0]$. Then $J - K = O(N^{-(2-p)})$ with the uniform mesh, $\tau_j = -j\frac{r}{N}$, and $J - K = O(N^{-2})$ with the graded mesh generated by (3.2.6).*

Proof. We shall use the notation $\tau_{j/2} := (\tau_{j-1} + \tau_j)/2$. Define $K_j := \frac{g_j}{\delta_j}(\varphi(t_{k+1},\tau_{j-1}) - \varphi(t_{k+1},\tau_j))$ and $J_j := \int_{\tau_j}^{\tau_{j-1}} g(\theta)\varphi_\theta(t_{k+1},\theta)d\theta$, $j = 1, 2, \ldots$, where we switched to the alternate notation $\varphi_\theta = \frac{\partial}{\partial\theta}\varphi$. Using straightforward calculations involving the Taylor series expansion of $\varphi(t_{k+1},\theta)$ with respect to its second argument around $\tau_{\frac{j}{2}}$ we obtain the estimate

$$\left|\frac{1}{\delta_j}\left(\varphi(t_{k+1},\tau_{j-1}) - \varphi(t_{k+1},\tau_j)\right) - \varphi_\theta(t_{k+1},\tau_{j/2})\right| \le M\delta_j^2,$$

where $M := \max_{[-r,0]}|\varphi_{\theta\theta\theta}(t_{k+1},s)|$ and therefore $\left|K_j - g_j\varphi_\theta(t_{k+1},\tau_{j/2})\right| \le M\delta_j^2 g_j$. Using the Taylor expansion around $\tau_{j/2}$ again, we have

$$J_j - g_j\varphi_\theta(t_{k+1},\tau_{j/2}) = \int_{\tau_j}^{\tau_{j-1}} (-\theta)^{-p}\left(\varphi_\theta(t_{k+1},\theta) - \varphi_\theta(t_{k+1},\tau_{j/2})\right)d\theta$$

$$= \varphi_{\theta\theta}(t_{k+1}, \tau_{j/2}) \int_{\tau_j}^{\tau_{j-1}} (-\theta)^{-p} \left(\theta - \tau_{j/2}\right) d\theta + \int_{\tau_j}^{\tau_{j-1}} (-\theta)^{-p} E(\theta) d\theta,$$

where $E(\theta) = \frac{1}{2}\varphi_{\theta\theta\theta}(t_{k+1}, \tilde{\tau}_{j/2})(\theta - \tau_{j/2})^2$ is the error term and $\tilde{\tau}_{j/2}$ is between θ and $\tau_{j/2}$. By the mean value theorem for integrals we have that $\left|\int_{\tau_j}^{\tau_{j-1}} (-\theta)^{-p} E(\theta) d\theta\right| = |E(\theta_j) g_j| \le M\delta_j^2 g_j$ where $\theta_j \in (\tau_j, \tau_{j-1})$. Denote $\xi_j = \tau_{j-1}/\delta_j$. In a fashion similar to Eggermont in [11], using the change of variables $y = (\theta - \tau_{j-1})/(\tau_j - \tau_{j-1})$ and repeated integration-by-parts we get that

$$\int_{\tau_j}^{\tau_{j-1}} \frac{\left(\theta - \tau_{j/2}\right)}{(-\theta)^p} d\theta = -\delta_j^{2-p} \int_0^1 \frac{y - 1/2}{(y - \xi_j)^p} dy$$

$$= \delta_j^{2-p} \left(\frac{p}{12}(1 - \xi_j)^{-p-1} + \int_0^1 p(p+1)(y - \xi_j)^{-p-2} \left(\frac{y^3}{6} - \frac{y^2}{4} \right) dy \right)$$

$$= \delta_j^{2-p} O((1 - \xi_j)^{-p-1})$$

as $-\xi_j \longrightarrow \infty$. Combining the previous two estimates we get $|J_j - g_j \varphi_\theta(t_{k+1}, \tau_{j/2})| \le C\delta_j^{2-p}(1 - \xi_j)^{-p-1} + M\delta_j^2 g_j$ for some constant C. Note that $J - K = \sum_{j=1}^N J_j - K_j$. Thus, denoting $h_j := g_j \varphi_\theta(t_{k+1}, \tau_{j/2})$, we get

$$|J - K| \le \sum_{j=1}^N |J_j - h_j| + |h_j - K_j| \le \sum_{j=1}^N C\delta_j^{2-p}(1 - \xi_j)^{-p-1} + 2M\delta_j^2 g_j. \tag{3.3.1}$$

If the mesh is uniform then $\delta_j = r/N$ and $\tau_j = -rj/N$ for all j. This gives that $(1 - \xi_j)^{-p-1} = j^{-p-1}$. Combining this with the fact that $\sum_{j=1}^N j^{-p-1} < \sum_{j=1}^\infty j^{-p-1} < \infty$, equation (3.3.1) gives that

$$|J - K| \le 2Mr^2 I N^{-2} + Cr^{2-p} N^{-(2-p)} \sum_{j=1}^N j^{-p-1} \le 2Mr^2 I N^{-2} + C' N^{-(2-p)},$$

where C' is some constant and $I := \int_{-r}^0 g(\theta) d\theta$. Thus $J - K = O(N^{-(2-p)})$ if the mesh is uniform.

If the mesh is graded then $g_j = I/N$ for all j and from this equation we get that $\tau_j = -rj^{\frac{1}{1-p}} N^{\frac{-1}{1-p}}$. For $b \ge -1$ and $\nu \ge 1$ the inequality $(1 + b)^\nu \ge 1 + \nu b$ holds true. Since $0 < 1 - p < 1$, this inequality gives that

$$\left(1 - \frac{1}{j}\right)^{\frac{1}{1-p}} \ge 1 - \frac{1}{(1-p)j}.$$

From the inequality immediately above we have that

$$\delta_j = r\left(\frac{j}{N}\right)^{\frac{1}{1-p}}\left[1-\left(1-\frac{1}{j}\right)^{\frac{1}{1-p}}\right] \le r\left(\frac{j}{N}\right)^{\frac{1}{1-p}}\frac{1}{j(1-p)} = aj^{\frac{p}{1-p}}N^{\frac{-1}{1-p}} =: \Delta_j, \tag{3.3.2}$$

where $a := r/(1-p)$. Note that $(1-\xi_j)^{-p-1} = \delta_j^{p+1}(-\tau_j)^{-p-1}$ and so

$$\delta_j^{2-p}(1-\xi_j)^{-p-1} = \delta_j^3(-\tau_j)^{-p-1} \le \Delta_j^3(-\tau_j)^{-p-1} = a'N^{-2-\frac{p}{1-p}}j^{-1+\frac{p}{1-p}}, \tag{3.3.3}$$

where $a' := r^{2-p}/(1-p)^3$. Recall that $\sum_{j=1}^{N} j^q = O(N^{q+1})$ for $q > -1$ and note $\delta_j \le \Delta_j \le \Delta_N = aN^{-1}$. Hence, from equations (3.3.1), (3.3.2), and (3.3.3), we get that

$$|J-K| \le 2MI\Delta_N^2 + Ca'N^{-2-\frac{p}{1-p}}\sum_{j=1}^{N} j^{-1+\frac{p}{1-p}} \le 2MIa^2N^{-2} + C''N^{-2-\frac{p}{1-p}}N^{\frac{p}{1-p}}$$

for some constant C''. Thus $J-K = O(N^{-2})$ if the mesh is graded.

□

Both claims in Lemma 3.3.1 are now established and show that the discretization error of $J-K$ converges to zero faster with the non-uniform graded mesh than with uniform mesh. Note that we do not always have the smoothness assumed here and the examples to follow will show that a discontinuity at zero in the derivatives of the true solution and the forcing function will also affect the rate of convergence. Also, although we only considered the case when $g(\theta) = |\theta|^{-p}$, it is believed that the graded mesh (3.2.6) improves the rate of convergence of the scheme even for more general kernels, e.g., g with the properties described in Section 3.1.

With Lemma 3.3.1 established, the question now is: how the improvement in the discretization error $J-K$ effects the actual (i.e., numerically observed) rate of convergence of the numerical schemes (3.2.12)? The purpose of the next section is to give a partial answer to this question by presenting case studies to illustrate the dependence of the actual rate of convergence of the fully-discrete implicit scheme on mesh selection.

3.4 Numerical examples

In this section we consider examples where we apply the aforementioned scheme (3.2.12) using both uniform and graded meshs. We first give a few words on what we mean by numerical rate of convergence.

We want to study the rate of convergence of the error function $e_N(t) := \varphi^N(t) - x(t)$ to zero where t will be taken to be a time-step node point. That is, we want to estimate a value $m > 0$ such that $|e_N(t)| \leq cN^{-m}$ as $N \to \infty$ and where $c > 0$ is a constant. Taking the logarithm of this inequality (assuming it is defined) we have $\log(|e_N(t)|) \leq \log(c)$ - $m\log(N) =: \ell(N)$. We can see that $\log(e_N(t))$ lies below $\ell(N)$ for all N after some N' and if we plot $\log(e_N(t))$ against $\log(N)$ (where $\log(N)$ is on the horizontal axis) as N increases we can conclude that the sequence $\log(e_N(t))$ decreases at a rate m' that is at least as fast as m. We can then use m' as our approximate rate of convergence of $|e_N(t)|$ to zero. With this idea in mind, in the examples to follow we will compute the approximate solution for $N = 10, 20, 40, 80, 160$, and 320 and plot the log of the errors against the $\log(N)$ to approximate the rate of convergence. In Examples 3.4.3 and 3.4.6 we instead consider the rate of convergence to zero of the maximum error $|e_N|_\infty := \max\{|e_N(t)| : t \in (0, 1]$ is a time-step node point$\}$ as N increases and apply this same idea.

When it is not apparent what the numerical rate of convergence is, e.g. see Figures 3.5, 3.6, and 3.7 in Example 3.4.5, we provide least-squares lines to approximate the rate of convergence. That is, for fixed t we provide a best fit function $ms+b$, where m and b are such that $\sum_{N \in A}[\log(e_N(t)) - (m\log(N) + b)]^2$, where $A := \{10, 20, 40, 80, 160, 320\}$, is minimized, i.e., m and b are such that $ms + b$ simultaneously minimizes the distance of each point $(\log(N), \log(e_N(t))$ to this line. This sum is a differentiable function of the two variables m and b and can thus be found using minimization techniques from standard calculus. A least-squares line will be considered to be the average numerical rate of convergence as the discretization in space is refined and it will itself be referred to as the numerical rate of convergence. These lines will be denoted as " – LS lines" in the figures.

Remark 3.4.1. In the examples to follow we take a weakly singular Volterra equation of the first kind and reformulate it into an equation of the form (3.1.1). For example, consider an equation of the form

$$\int_0^t g(t-s)x(s)ds = f(t), \tag{3.4.1}$$

where $f(0) = 0$, $f'(t)$ is locally integrable, and x is the unknown function to be determined. Letting $\theta = -(t-s)$ we have that $\int_0^t g(t-s)x(s)ds = \int_{-t}^0 g(-\theta)x(t+\theta)d\theta$ and, in addition, if we define $x(u) = 0$ for $u \leq 0$ then

$$\int_0^t g(t-s)x(s)ds = \int_{-r}^{-t} g(-\theta)x(t+\theta)d\theta + \int_{-t}^0 g(-\theta)x(t+\theta)d\theta = \int_{-r}^0 g(-\theta)x(t+\theta)d\theta.$$

Thus, after differentiating, (3.4.1) can be reformulated to take the form

$$\begin{aligned} \frac{d}{dt}\left(\int_{-r}^0 g(-\theta)x(t+\theta)d\theta\right) &= f'(t) \text{ for } t > 0, r > 0, \\ \text{with } x(\theta) &= 0 \text{ for } -r \leq \theta \leq 0. \end{aligned} \tag{3.4.2}$$

We shall use $T = 1$ and $r = 1$ in the examples to follow. ■

Example 3.4.1. Consider first the following example given in the text [37] on integral equations by A.M. Wazwaz,

$$\int_0^t \frac{x(s)}{(t-s)^{1/4}}ds = \frac{128}{231}t^{11/4}.$$

Reformulated, this equation can be stated as

$$\frac{d}{dt}\left(\int_{-1}^0 \frac{x(t+\theta)}{|\theta|^{1/4}}d\theta\right) = \frac{32}{21}t^{7/4}$$

Table 3.1. Example 3.4.1. Graded error table. $\Delta t = 1/N$.

mesh↓ time→	0.2	0.4	0.6	0.8
10	0.001013657	0.001353132	0.001610427	0.001854214
20	0.000272433	0.000357831	0.000423953	0.000479526
40	7.15E-05	9.33E-05	0.000110144	0.000124464
80	1.85E-05	2.41E-05	2.84E-05	3.20E-05
160	4.76E-06	6.16E-06	7.25E-06	8.17E-06
320	1.21E-06	1.57E-06	1.84E-06	2.08E-06

Table 3.2. Example 3.4.1. Uniform error table. $\Delta t = 1/N$.

mesh↓ time→	0.2	0.4	0.6	0.8
10	0.002077632	0.002830702	0.003326358	0.003706897
20	0.000707676	0.000926724	0.001072235	0.001184404
40	0.000231681	0.000296101	0.00033911	0.000372326
80	7.40E-05	9.31E-05	0.000105834	0.000115691
160	2.33E-05	2.89E-05	3.27E-05	3.56E-05
320	7.23E-06	8.91E-06	1.00E-05	1.09E-05

for $t > 0$ and $x(t) = 0$ for $t \leq 0$. The true solution is $x(t) = t^2$. The graded mesh is given by $\{\tau_j\}$ where

$$\int_{\tau_j}^{\tau_{j-1}} |\theta|^{-1/4} d\theta = \frac{1}{N} \int_{-1}^{0} |\theta|^{-1/4} d\theta \tag{3.4.3}$$

for $j \geq 1$. In Figure 3.1, we plot $\log_2(e_N(t = 0.4))$ against $\log_2(N)$ with $\Delta t = 1/N$ as N increases. We see that the convergence rate at $t = 0.4$ is approximately 1.9 for the graded mesh and approximately 1.6 for the uniform mesh. Compare these to the expected rates of 2 and 1.75, for graded and uniform mesh, respectively. From Tables 3.1–3.2 we can see that accuracy is also better with graded mesh under most mesh sizes.

Example 3.4.2. This example is given in [33] where Rahman et al. study numerical solutions of first and second kind weakly singular Volterra equations using Laguerre polynomials,

$$\int_0^t \frac{x(s)}{(t-s)^{1/2}} ds = t^5.$$

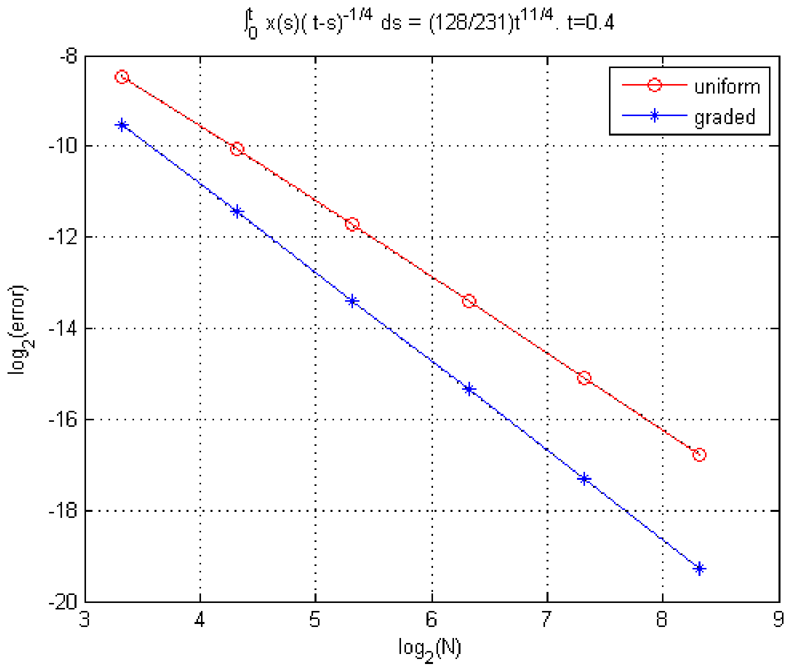

Figure 3.1. Example 3.4.1. Approximate rates of convergence for both meshes at $t = 0.4$.

Reformulated, this equation can be stated as

$$\frac{d}{dt}\left(\int_{-1}^{0} \frac{x(t+\theta)}{|\theta|^{1/2}} d\theta\right) = 5t^4$$

for $t > 0$ and $x(t) = 0$ for $t \leq 0$. The true solution is $x(t) = \frac{1280}{315\pi}t^{9/2}$.

From Tables 3.3–3.4 we can see that accuracy is increased at most time-steps shown for the graded mesh. Furthermore, from Figure 3.2, we can see also see that at $t = 0.6$ the rate of convergence is about 1.45 for uniform mesh and about 2 for graded mesh.

Example 3.4.3. The following example was also found in the text [37]. Consider

$$\int_0^t \frac{x(s)}{(t-s)^{1/2}} ds = \frac{8}{3}t^{3/2} + \frac{16}{5}t^{5/2}.$$

Reformulated, this equation can be stated as

$$\frac{d}{dt}\left(\int_{-1}^{0} \frac{x(t+\theta)}{|\theta|^{1/2}} d\theta\right) = 4t^{1/2} + 8t^{3/2}$$

Table 3.3. Example 3.4.2. Graded error table. $\Delta t = 1/N$.

mesh↓ time→	0.2	0.4	0.6	0.8
10	0.000170697	0.001140789	0.003566658	0.008178993
20	4.40E-05	0.000287571	0.000895002	0.002046136
40	1.11E-05	7.20E-05	0.000223952	0.000511856
80	2.78E-06	1.80E-05	5.60E-05	0.000127977
160	6.95E-07	4.51E-06	1.40E-05	3.20E-05
320	1.74E-07	1.13E-06	3.50E-06	8.00E-06

Table 3.4. Example 3.4.2. Uniform error table. $\Delta t = 1/N$.

mesh↓ time→	0.2	0.4	0.6	0.8
10	0.000385704	0.003632379	0.01320325	0.032723612
20	0.00016053	0.001446193	0.00514585	0.012585171
40	6.39E-05	0.000556191	0.001947204	0.004715879
80	2.46E-05	0.000208414	0.000721241	0.00173485
160	9.21E-06	7.67E-05	0.000263218	0.000630195
320	3.39E-06	2.79E-05	9.51E-05	0.000226974

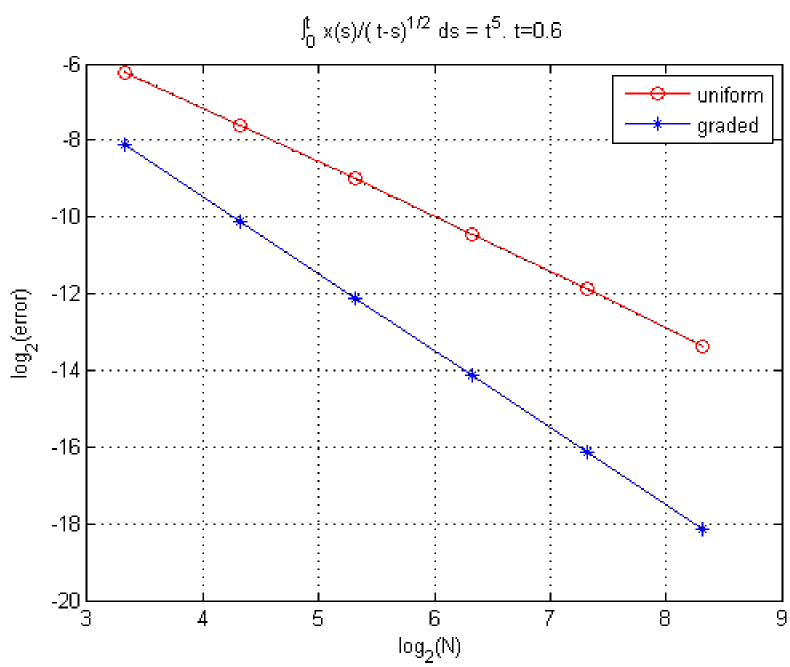

Figure 3.2. Example 3.4.2. Approximate rates of convergence for both meshes at $t = 0.6$.

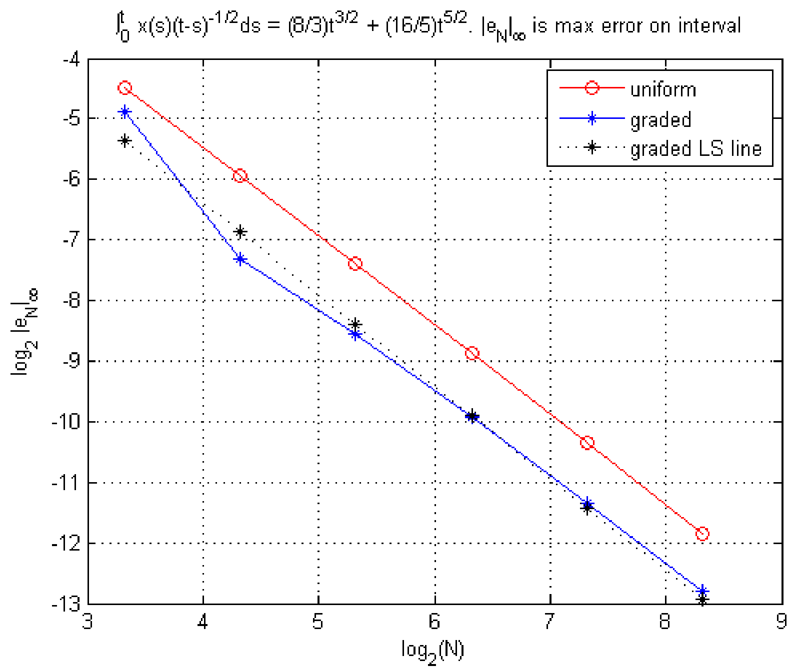

Figure 3.3. Example 3.4.3. Approximate rates of convergence in the max error on $(0, 1]$.

for $t > 0$ and $x(t) = 0$ for $t \leq 0$. The true solution is $x(t) = 2t + 3t^2$.

In this example, we look at the convergence to the true solution in the max error $|e_N|_\infty$ as N increases. The max error was chosen here so that we can get an understanding of the error on the whole interval and not only at a fixed time. From Figure 3.3 we can estimate that the max error rate of convergence is about 1.5 for both uniform and graded mesh with $\Delta t = 1/N$. Unlike the first two examples, note that the forcing function in the reformulated equation has an unbounded derivative at zero. It seems that this discontinuity may have compromised the expected rate of convergence of 2 for the graded mesh. From Tables 3.5–3.6 we can see that the accuracy appears to be better for the graded mesh.

Example 3.4.4. The following example was found in [20], where S. Jahanshahi et al. considered a numerical method to solve Abel integral equations of the first kind. Consider

Table 3.5. Example 3.4.3. Graded error table. $\Delta t = 1/N$.

mesh↓ time→	0.2	0.4	0.6	0.8
10	0.009505526	0.004760497	0.000962417	0.00126726
20	0.004514347	0.002602599	0.001423843	0.001190168
40	0.001852882	0.001142082	0.000758405	0.000998067
80	0.000711964	0.000457861	0.000329369	0.000379532
160	0.000264705	0.000175193	0.000131781	0.000138337
320	9.66E-05	6.52E-05	5.04E-05	4.77E-05

Table 3.6. Example 3.4.3. Uniform error table. $\Delta t = 1/N$.

mesh↓ time→	0.2	0.4	0.6	0.8
10	0.016568542	0.026032073	0.033280012	0.039371411
20	0.006508018	0.009842853	0.012389938	0.014532092
40	0.002460713	0.003633023	0.004529736	0.00528466
80	0.000908256	0.001321165	0.001637446	0.00190389
160	0.000330291	0.000475972	0.000587655	0.000681773
320	0.000118993	0.000170443	0.000209904	0.000243164

$$\int_0^t \frac{x(t)}{(t-s)^{1/2}} ds = e^t - 1.$$

Reformulated, this equation can be stated as

$$\frac{d}{dt}\left(\int_{-1}^{0} \frac{x(t+\theta)}{|\theta|^{1/2}} d\theta\right) = e^t$$

for $t > 0$ and $x(t) = 0$ for $t \leq 0$. The true solution is given by

$$x(t) = \frac{e^t}{\sqrt{\pi}} erf(\sqrt{t}),$$

where $erf(u) = \frac{2}{\sqrt{\pi}} \int_0^u e^{-t^2} dt$ is the error function.

At $t = 0.4$, Figure 3.4 shows that the uniform mesh and the graded mesh yield rates of convergence of approximately 1 and 0.66, respectively, for the given range of mesh sizes. We can see that uniform mesh performed better, however, both rates are slower than expected. These slow rates of convergence are not surprising since the true solution has unbounded derivatives at zero. Figure 3.4 and Tables 3.7–3.8 show that there is a significant increase in

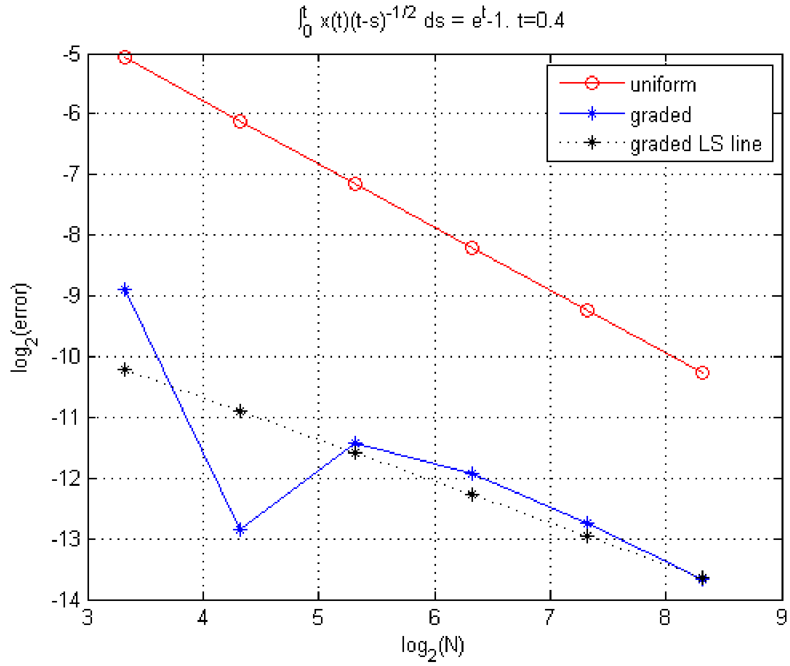

Figure 3.4. Example 3.4.4. Approximate rates of convergence for both meshes at $t = 0.4$.

Table 3.7. Example 3.4.4. Graded error table. $\Delta t = 1/N$.

mesh↓ time→	0.2	0.4	0.6	0.8
10	0.000370818	0.002113945	0.003781737	0.00386041
20	0.002143661	0.00013414	0.000542405	0.003049412
40	0.001550951	0.000363341	7.40E-06	0.000872734
80	0.000890558	0.000254809	6.73E-05	0.000370849
160	0.00047324	0.000145548	4.96E-05	0.000116045
320	0.000243497	7.73E-05	2.88E-05	8.89E-06

accuracy with graded mesh.

Example 3.4.5. Now consider the following example found in [19],

$$\frac{1}{\sqrt{\pi}}\int_0^t \frac{e^{-(t-s)}}{(t-s)^{1/2}}x(s)ds = e^{-t}(t+t^3+t^5).$$

Table 3.8. Example 3.4.4. Uniform error table. $\Delta t = 1/N$.

mesh↓ time→	0.2	0.4	0.6	0.8
10	0.039093198	0.030079998	0.026815735	0.025626279
20	0.019228306	0.014461254	0.01263222	0.011821375
40	0.009444242	0.006989921	0.006006089	0.005521185
80	0.004651519	0.003401174	0.002884524	0.002613131
160	0.002298403	0.00166528	0.001398143	0.001252004
320	0.001138937	0.000819623	0.000682923	0.00060611

Reformulated, this equation can be stated as

$$\frac{d}{dt}\left(\int_{-1}^{0} \frac{e^{\theta}}{|\theta|^{1/2}} x(t+\theta)d\theta\right) = \sqrt{\pi}(-e^{-t}(t+t^3+t^5) + e^{-t}(1+3t^2+5t^4))$$

for $t > 0$ and $x(t) = 0$ for $t \leq 0$. The true solution is given by

$$x(t) = e^{-t}\left(\frac{\Gamma(2)}{\Gamma(3/2)}t^{1/2} + \frac{\Gamma(4)}{\Gamma(7/2)}t^{5/2} + \frac{\Gamma(6)}{\Gamma(11/2)}t^{9/2}\right).$$

Note that the true solution has unbounded derivatives at zero.

It is reasonable to expect the scheme to be more accurate as Δt gets smaller. Hence, the purpose of this example is to study how the rate of convergence at different times is affected when we consider time-steps smaller than $\Delta t = 1/N$. The size of system (3.2.12) does not change when we decrease the step-size since the discretization of $[-1, 0]$ remains fixed.

We note that the kernel gives difficulty in extracting a graded mesh tailored to this particular equation. Instead we use the mesh we get by ignoring the exponential part, i.e., the mesh generated using kernel $g(\theta) = |\theta|^{-1/2}$, since the strength of the singularity at zero is similar for both kernels.

At $t = 0.2$, Figure 3.5 suggests that the rate of convergence is approximately 0.5 with $\Delta t = 1/N$, and if we decrease the step-size to $1/(2N)$ the rate increases to approximately 2.1 and then decreases to approximately 1.96 for $1/(4N)$. Figure 3.6 shows the approximate convergence rates at $t = 0.6$ to be 1.68, 1.86, and 1.66 for $\Delta t = 1/N, 1/(2N)$, and $1/(4N)$, respectively. In Figure 3.7 we see that the rate does not improve when we decrease the

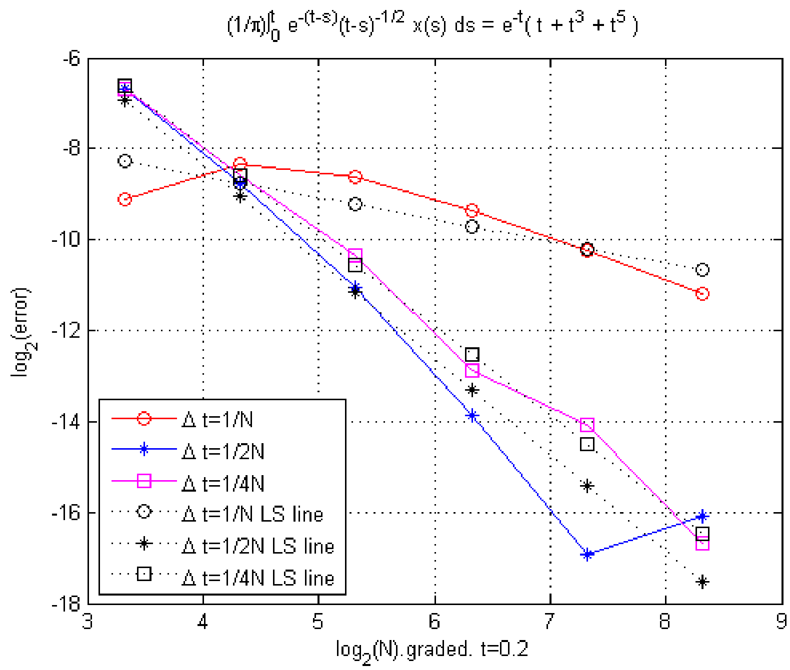

Figure 3.5. Example 3.4.5. Approximate rates of convergence with graded mesh at $t = 0.2$.

step-size at $t = 0.8$ where the convergence rates are approximately 1.95, 0.96, and 1.3 for $\Delta t = 1/N, 1/(2N)$, and $1/(4N)$, respectively. Although there were improvements at $t = 0.2$ and $t = 0.6$ with $\Delta t = 1/(2N)$, it was not as beneficial with $\Delta t = 1/(4N)$. There was no such improvement at $t = 0.8$. We can conclude that decreasing the time step size can help restore the rates of convergence, however, not uniformly on $(0, 1]$. The discontinuities in the derivatives of the true solution at zero may have influenced the numerical results.

Example 3.4.6. We now give an example of a problem where the numerical solution performs better with uniform mesh, see again [37]. Consider

$$\int_0^t \frac{x(s)}{(t-s)^{1/2}} ds = \frac{4}{3} t^{3/2}.$$

Reformulated, this equation can be stated as

$$\frac{d}{dt}\left(\int_{-1}^{0} \frac{x(t+\theta)}{|\theta|^{1/2}} d\theta\right) = 2t^{1/2}$$

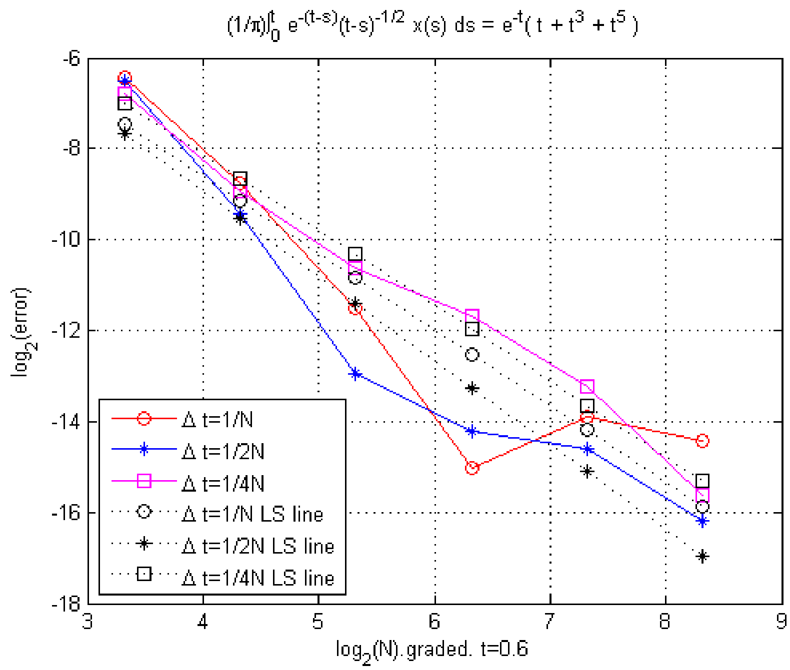

Figure 3.6. Example 3.4.5. Approximate rates of convergence with graded mesh at $t = 0.6$.

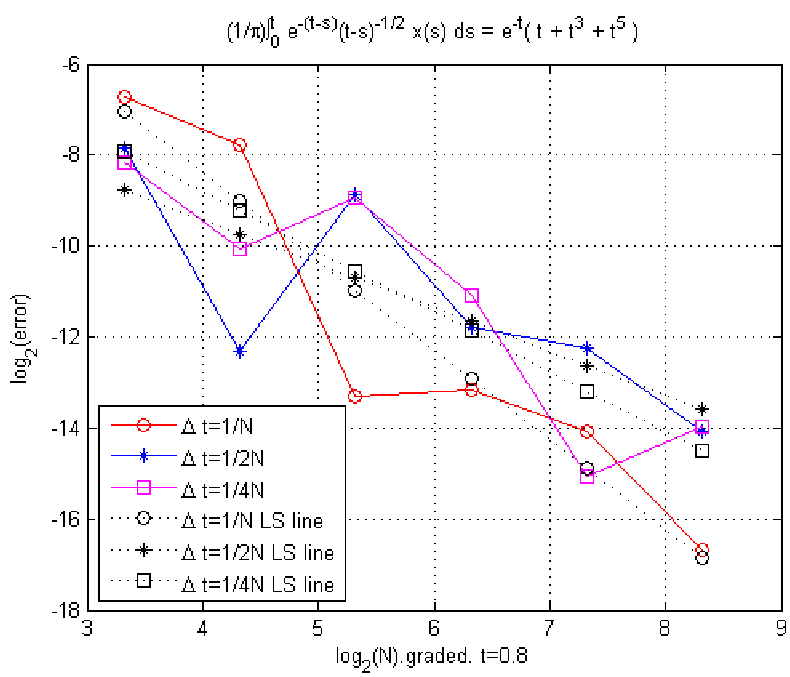

Figure 3.7. Example 3.4.5. Approximate rates of convergence with graded mesh at $t = 0.8$.

for $t > 0$ and $x(t) = 0$ for $t \leq 0$. The true solution is $x(t) = t$.

From Table 3.9 note that the error for the uniform mesh is near zero at the times shown. In fact, it seems that under the uniform mesh the scheme produces the exact solution. This is suspected to be related to the slope of the characteristic lines (see Remark 3.2.1) being the same as the (negative) slope of the true solution and the fact that the uniform mesh scheme computes the numerical solution along these characteristic lines. For the graded mesh, Figure 3.8 suggests that we get a convergence rate in the max error of about 1.5.

Table 3.9. Example 3.4.6. Uniform error table. $\Delta t = 1/N$.

mesh↓ time→	0.2	0.4	0.6	0.8
10	2.78E-17	0	1.11E-16	0
20	0	0	1.11E-16	0
40	0	0	1.11E-16	2.22E-16
80	0	0	3.33E-16	4.44E-16
160	5.55E-17	1.67E-16	2.22E-16	1.11E-15
320	1.11E-16	4.44E-16	4.44E-16	0

Table 3.10. Example 3.4.6. Graded error table. $\Delta t = 1/N$.

mesh↓ time→	0.2	0.4	0.6	0.8
10	0.006575578	0.004990873	0.003880048	0.004728787
20	0.002724213	0.001962718	0.001565912	0.000529
40	0.001045101	0.000738097	0.000593916	0.000751729
80	0.000386044	0.000271026	0.00021865	0.000254528
160	0.000139948	9.82E-05	7.94E-05	8.55E-05
320	5.02E-05	3.53E-05	2.86E-05	2.80E-05

Example 3.4.7. As a final application of graded meshes, we consider an example where the dependent variable, $x(t)$, also appears in the right side of the equation. Consider

$$\frac{d}{dt}\left(\int_{-1}^{0} \frac{x(t+s)}{|s|^{1/2}} ds\right) = x(t) - t^6 + \frac{1024}{231} t^{11/2}$$

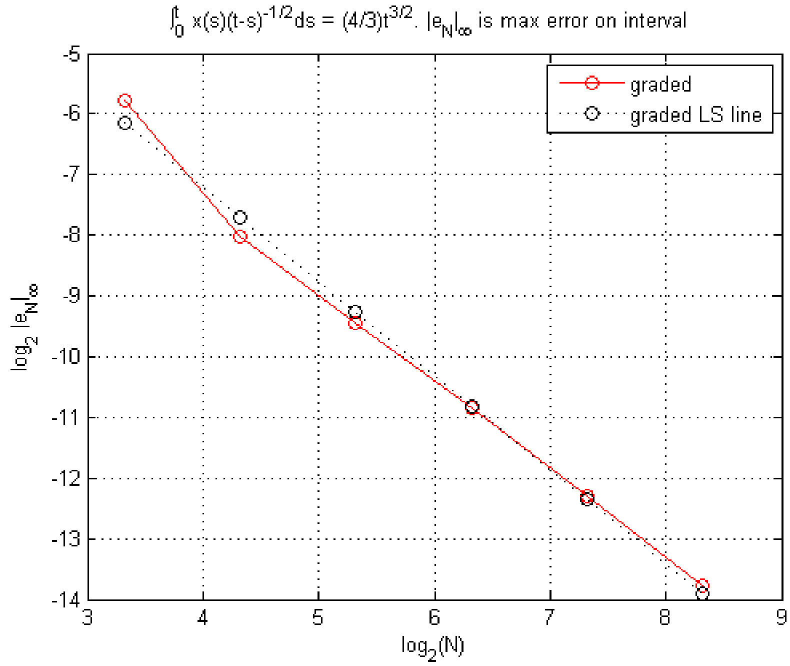

Figure 3.8. Example 3.4.6. Approximate rate of convergence in the max error on (0,1].

for $t > 0$ and $x(u) = 0$ for $u \leq 0$. The true solution is $x(t) = t^6$. This requires only a minor modification in the discretization of the boundary condition. More explicitely, if we recall the notation of Section 3.2, the discretized boundary condition (3.2.11) has the modified form $-\alpha_0^{k+1} + \sum_{j=1}^{N} g_j(\alpha_{j-1}^{k+1} - \alpha_j^{k+1})/\delta_j = f^{k+1}$. From Figure 3.9, we get a numerical convergence rate of about 1.5 for uniform mesh and 2 for graded mesh at time $t = 0.4$.

Table 3.11. Example 3.4.7. Uniform error table. $\Delta t = 1/N$.

mesh↓ time→	0.2	0.4	0.6	0.8
10	4.48E-05	0.001267769	0.008851268	0.035107414
20	1.86E-05	0.000504024	0.003454789	0.013542525
40	7.45E-06	0.000195381	0.001317837	0.005114189
80	2.89E-06	7.39E-05	0.000492225	0.001895588
160	1.10E-06	2.74E-05	0.000180854	0.000692665
320	4.07E-07	1.00E-05	6.57E-05	0.000250544

To conclude this section we illustrate the flexibility of this scheme by applying it to a scalar delay differential equation.

Table 3.12. Example 3.4.7. Graded error table. $\Delta t = 1/N$.

mesh↓ time→	0.2	0.4	0.6	0.8
10	2.28E-05	0.00046216	0.00271248	0.009714935
20	6.17E-06	0.00011739	0.000681765	0.002432978
40	1.57E-06	2.95E-05	0.000170666	0.000608517
80	3.94E-07	7.37E-06	4.27E-05	0.000152146
160	9.87E-08	1.84E-06	1.07E-05	3.80E-05
320	2.47E-08	4.61E-07	2.67E-06	9.51E-06

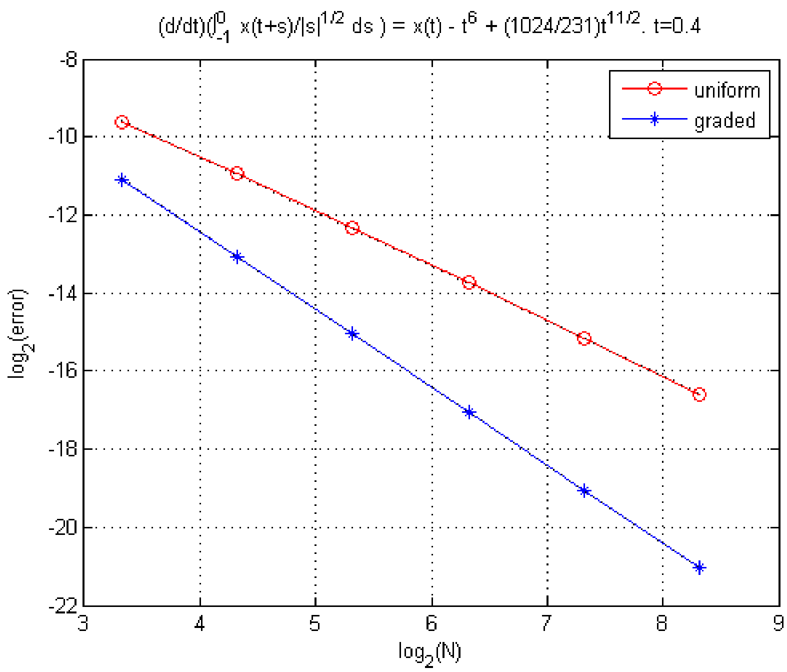

Figure 3.9. Example 3.4.7. Approximate rates of convergence for both meshes at $t = 0.4$.

Example 3.4.8. The following scalar delay differential equation was studied in [2]. Consider

$$\dot{x}(t) = 5x(t) + x(t-1) \tag{3.4.4}$$

with initial data

$$x(t) = 5, t \in [-1, 0].$$

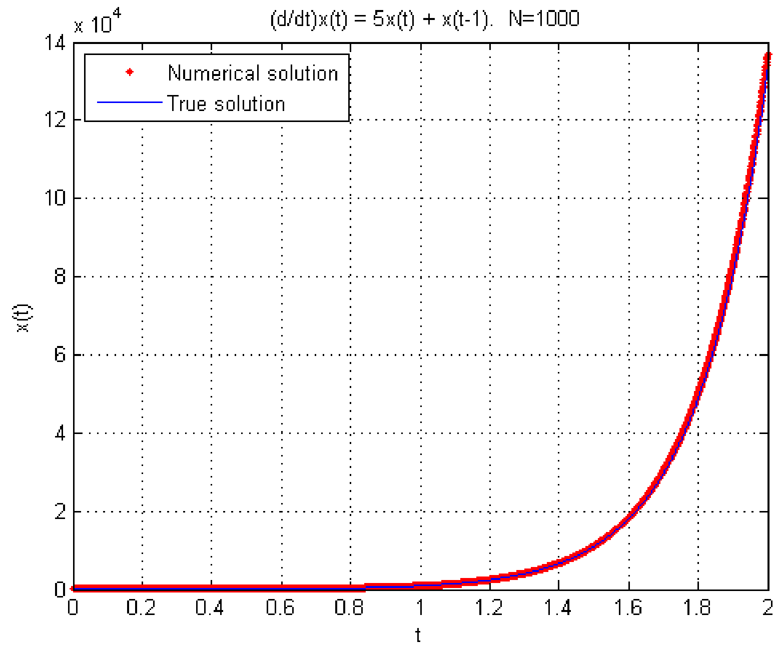

Figure 3.10. Example 3.4.8. Approximate solution for a scalar DDE.

The true solution on $[0, 2]$ is given by

$$x(t) = \begin{cases} 6e^{5t} - 1 & 0 \leq t \leq 1 \\ (x(1) - \frac{1}{5} + 6(t-1))e^{5(t-1)} + \frac{1}{5} & 1 \leq t \leq 2 \end{cases}.$$

The associated scheme, with $\Delta t = \delta$, is given by

$$\alpha_j^{k+1} = \alpha_{j-1}^k$$

for $j = 1, 2, \ldots, N$. Substituting $\varphi^N(t, \theta)$, as defined above, into the delay equation yields the boundary condition

$$\alpha_0^{k+1}(\frac{1}{\delta} - 5) - \alpha_1^{k+1}\frac{1}{\delta} - \alpha_N^{k+1} = 0.$$

Figure 3.10 shows the numerical solution generated by this scheme.

3.5 Conclusions

The "degradation" in rate of convergence for SNFDEs with weakly singular kernels was observed in [19] (when using uniform meshes) and in this chapter we investigated possible fixes of this phenomenon. In particular, we considered graded meshes (where grading was related to the strength of the singularity of the kernel function in the SNFDE under consideration) to improve on the rate of convergence. In Section 3.3, we established that the graded mesh is a viable alternative to uniform mesh and in Section 3.4 we applied it to concrete examples. Examples 3.4.1 and 3.4.2 indeed show that the expected rate of convergence of 2 can be recovered if the graded mesh is applied. However, Examples 3.4.3 and 3.4.4 show that discontinuities in the derivatives of either the forcing function or the true solution may compromise the expected rates of convergence. We note that in all the Examples 3.4.1–3.4.4 accuracy improved at most of the time-steps shown with graded mesh. Finally, we showed the flexibility of the scheme by applying it to a delay differential equation.

CHAPTER 4

APPROXIMATIONS FOR SINGULAR NEUTRAL FUNCTIONAL DIFFERENTIAL EQUATION SYSTEMS

NFDEs and SNFDEs are inherently infinite-dimensional problems, i.e., we are looking for a solution in an infinite-dimensional function space. Methods for solving NFDEs are typically extensions from methods first developed to solve RFDEs. These methods typically involve approximating the original NFDE by a sequence of finite-dimensional ordinary differential equations. See, for example, [1], where the method of averaging projections is introduced to solve RFDEs numerically. This method was then applied in the case of NFDEs and SNFDEs, e.g., in [21] and [19], respectively. The fact that we are approximating an infinite-dimensional problem by a finite-dimensional problem is important for computational purposes.

In the previous chapter we considered numerical approximations for certain scalar SNFDEs. In this chapter we will consider the extension to the system case. Namely, we will consider numerical approximations of the system (2.4.1)–(2.4.3) and provide a preliminary numerical case study on its stabilizability.

4.1 A Numerical Scheme

We now construct a numerical scheme for the SNFDE

$$\frac{d}{dt}\left(x(t) + \int_{-r}^{0} a_{12}(s)y_t(s)ds\right) = b_{11}x(t) + b_{12}y_t(0) + \int_{-r}^{0} b_{12}(s)y_t(s)ds + f(t) \tag{4.1.1}$$

$$\frac{d}{dt}\left(\int_{-r}^{0} g(s)y_t(s)ds\right) = b_{21}x(t) \tag{4.1.2}$$

with initial condition

$$x(0) = \eta, \quad y_0(s) = \rho(s),$$

where $y_t(s) := y(t+s)$ for $s \in [-r, 0]$ and $t \geq 0$. Here, $a_{12}(s)$ and $b_{12}(s)$ are integrable functions and b_{11} and b_{12} are scalars. Also the kernel $g(s)$, $-r \leq s < 0$, is positive, monotonically increasing, integrable on $[-r, 0]$, with $g(s) \longrightarrow \infty$ as $s \longrightarrow 0^-$.

We again proceed as in [16] and [19] and convert the SNFDE (4.1.1)-(4.1.2) into a first order hyperbolic partial differential equation with nonlocal boundary conditions. The initial data at $t = 0$ is given by the initial function $\rho(s)$, $-r \leq s \leq 0$. Define $\varphi(t,s) := y(t+s)$ for $-r < s < 0$ and $t \geq 0$. Assuming that φ is differentiable it satisfies the PDE

$$\frac{\partial}{\partial t}\varphi(t,s) = \frac{\partial}{\partial s}\varphi(t,s), \tag{4.1.3}$$

for $t \geq 0$, $-r < s < 0$. Furthermore, it follows from (4.1.3) that the system (4.1.1)–(4.1.2) for $t > 0$ can be written as

$$\frac{d}{dt}x(t) + \int_{-r}^{0} a_{12}(s)\frac{\partial}{\partial s}\varphi(t,s)ds = b_{11}x(t) + b_{12}\varphi(t,0) + \int_{-r}^{0} b_{12}(s)\varphi(t,s)ds + f(t) \tag{4.1.4}$$

and

$$\int_{-r}^{0} g(\theta)\frac{\partial}{\partial s}\varphi(t,\theta)d\theta = b_{21}x(t). \tag{4.1.5}$$

For convenience, we restate the approximating function. Let N be a positive integer and introduce the partition of the interval $[-r, 0]$ as $-r =: \tau_N < \tau_{N-1} < \cdots < \tau_1 < \tau_0 := 0$ and let $\delta_j := \tau_{j-1} - \tau_j > 0$ for $1 \leq j \leq N$. We again use the approximating function

$$\varphi^N(t,\theta) := \sum_{j=0}^{N} \alpha_j(t)B_j(\theta) \text{ for } t \geq 0, -r \leq \theta \leq 0, \tag{4.1.6}$$

where the piecewise linear functions, B_j^N, $j = 0, 1, 2, ..., N$ are given as

$$B_j^N(\theta) := \begin{cases} (\theta - \tau_{j+1}^N)/\delta_{j+1}^N & \theta \in [\tau_{j+1}^N, \tau_j^N], \\ (\tau_{j-1}^N - \theta)/\delta_j^N & \theta \in [\tau_j^N, \tau_{j-1}^N], \\ 0 & \textit{otherwise} \end{cases} \text{ for } j = 1, 2, ..., N-1, \tag{4.1.7}$$

$$B_0^N(\theta) := \begin{cases} (\theta - \tau_1^N)/\delta_1^N & \theta \in [\tau_1^N, \tau_0^N], \\ 0 & otherwise \end{cases}, \tag{4.1.8}$$

and

$$B_N^N(\theta) := \begin{cases} (\tau_{N-1}^N - \theta)/\delta_N^N & \theta \in [\tau_N^N, \tau_{N-1}^N], \\ 0 & otherwise \end{cases}, \tag{4.1.9}$$

and $\alpha_j^N(t)$, $j = 0, 1, 2, ..., N$ are time dependent coefficients. Assume that a mesh is specified and consider a second-order space discretization to equation (4.1.3) (see [19]):

$$\frac{d}{dt}\left(\frac{\alpha_{j-1}(t) + \alpha_j(t)}{2}\right) = \frac{1}{\delta_j}(\alpha_{j-1}(t) - \alpha_j(t)) \tag{4.1.10}$$

for $1 \leq j \leq N$. Substituting $\varphi^N(t, \theta)$ into the equations (4.1.4)–(4.1.5) to advance the solution, we obtain

$$\begin{aligned} \frac{d}{dt}x(t) + \sum_{j=1}^{N} \frac{a_{12j}}{\delta_j}\left(\alpha_{j-1}(t) - \alpha_j(t)\right) &= b_{11}x(t) + b_{12}\alpha_0(t) \\ +\sum_{j=1}^{N}\left(b_{12j}\alpha_j(t) + \frac{\bar{b}_{12j}}{\delta_j}\left(\alpha_{j-1}(t) - \alpha_j(t)\right)\right) &+ f(t), \end{aligned} \tag{4.1.11}$$

and

$$\sum_{j=1}^{N} \frac{g_j}{\delta_j}(\alpha_{j-1}(t) - \alpha_j(t)) = b_{21}x(t), \tag{4.1.12}$$

where $g_j := \int_{\tau_j}^{\tau_{j-1}} g(\theta)d\theta$, $a_{12j} := \int_{\tau_j}^{\tau_{j-1}} a_{12}(s)ds$, $b_{12j} := \int_{\tau_j}^{\tau_{j-1}} b_{12}(s)ds$, and $\bar{b}_{12j} := \int_{\tau_j}^{\tau_{j-1}} sb_{12}(s)ds$. Equations (4.1.10)-(4.1.12) form the semi-discrete scheme. Using the second-order implicit trapezoidal rule in time in (4.1.10), we get the fully discretized scheme

$$\frac{1}{\Delta t}\left(\frac{\alpha_{j-1}^{k+1} + \alpha_j^{k+1}}{2} - \frac{\alpha_{j-1}^{k} + \alpha_j^{k}}{2}\right) = \frac{1}{2\delta_j}\left(\alpha_{j-1}^{k+1} - \alpha_j^{k+1} + \alpha_{j-1}^{k} - \alpha_j^{k}\right), \tag{4.1.13}$$

or, equivalently,

$$\alpha_{j-1}^{k+1}C_j + \alpha_j^{k+1} = \alpha_{j-1}^{k} + \alpha_j^{k}C_j, \tag{4.1.14}$$

where $C_j := \left(\frac{1}{\Delta t} - \frac{1}{\delta_j}\right) / \left(\frac{1}{\Delta t} + \frac{1}{\delta_j}\right)$. Define $t_{k/2} := (t_k + t_{k-1})/2$. Expanding $x(t)$ about $t_{k/2}$ we arrive at

$$\frac{1}{\Delta t}(x(t_{k+1}) - x(t_k)) = \dot{x}(t_{k/2}) + O((\Delta t)^2),$$

i.e., we a have the symmetric difference approximation for $\dot{x}(t)$ at $t_{k/2}$. Denote $h_j(t) := \alpha_{j-1}(t) - \alpha_j(t)$ and assume the coefficients $\alpha_j(t)$ are twice continuously differentiable for $t > 0$. Consider the Taylor expansions of $h_j(t)$ about $t_{k/2}$

$$h_j^{k+1} = h_j^{k/2} + \frac{\Delta t}{2} h_{t,j}^{k/2} + O((\Delta t)^2)$$

and

$$h_j^k = h_j^{k/2} - \frac{\Delta t}{2} h_{t,j}^{k/2} + O((\Delta t)^2).$$

Adding these two equations and rearranging the terms we arrive at

$$\frac{h_j^{k+1} + h_j^k}{2} = h_j^{k/2} + O((\Delta t)^2).$$

Using these approximations in the numerical boundary condition (4.1.11) we have

$$\begin{aligned}\frac{1}{\Delta t}\left(x^{k+1} - x^k\right) + \sum_{j=1}^{N} \frac{a_{12j}}{2\delta_j}\left(\alpha_{j-1}^{k+1} - \alpha_j^{k+1} + \alpha_{j-1}^k - \alpha_j^k\right) &= b_{11}x^{k+1} + b_{12}\alpha_0^{k+1} \\ + \sum_{j=1}^{N}\left(b_{12j}\alpha_j^{k+1} + \frac{\bar{b}_{12j}}{2\delta_j}\left(\alpha_{j-1}^{k+1} - \alpha_j^{k+1} + \alpha_{j-1}^k - \alpha_j^k\right)\right) &+ f^{k+1},\end{aligned} \tag{4.1.15}$$

where x^k is the approximation for $x(t_k)$. Finally, the fully discretized version of the equation (4.1.12) is given by

$$\sum_{j=1}^{N} \frac{g_j}{\delta_j}(\alpha_{j-1}^{k+1} - \alpha_j^{k+1}) = b_{21}x^{k+1}. \tag{4.1.16}$$

In this section we stated an approximation scheme for the SNFDE (4.1.1)–(4.1.2). In the next section we establish convergence of this scheme.

4.2 Convergence

In this section we establish the convergence of the scheme directly. By convergence of $\{x^k\}$ and $\{\alpha_j^k\}$, we mean that

$$|x(t_k) - x^k| \longrightarrow 0$$

and

$$\max_{0 \le j \le N} |\alpha_j^k - \varphi(t_k, \tau_j)| \longrightarrow 0,$$

as $\Delta t, \delta_j \longrightarrow 0$, where $x(t)$ and $\varphi(t,s)$ $(= y(t+s))$ are the true solutions. For $u \in \mathbb{R}^{N+1}$ denote

$$\|u\|_{\max} := \max_{0 \le j \le N} \{|u_j|\}.$$

We will consider the convergence under a mesh dependent scaled norm. We will assume that the true solutions are sufficiently differentiable to accomodate a Taylor series approach for convergence. Define $\varepsilon^k := x(t_k) - x^k$, $e_j^k := \alpha_j^k - \varphi_j^k$, $e^k := (e_0^k, e_1^k, \ldots, e_N^k)^T$, and let $\delta_j = \delta$ for all j. We will consider the special case where $\delta = \Delta t$.

Lemma 4.2.1. Let N be a positive integer, $T > 0$, $g(\theta) = |\theta|^{-p}$, $0 < p < 1$, for $\theta \in [-r, 0)$, $r > 0$, $f \in C^1[0,T]$, a_{12} and b_{12} are in $C^1[-r, 0]$, and assume that $x(t)$ and $\varphi(t,s) := y_t(s)$, $-r \le s \le 0$, are solutions to (4.1.4)–(4.1.5) with $x \in C^3[0,T]$ and $\varphi(t,\cdot) \in C^3[-r,0]$, $0 \le t \le T$. Additionally, we assume that the mesh is uniform in both space and time with $\Delta t = \delta$. Then, for $k+1 \le T/(\Delta t)$ and for some constant $C > 0$, $e^{-CN^{1-p}}[|\varepsilon^{k+1}| + \|e^{k+1}\|_{\max}] = O(\delta^{2-p})$.

Proof. For the function φ, define the discretization operators $P^{k/2,\Delta t}$ and $P_{j/2,\delta_j}$ as

$$P^{k/2,\Delta t}\varphi := \frac{1}{2\Delta t}\left(\varphi_{j-1}^{k+1} + \varphi_j^{k+1} - \varphi_{j-1}^k - \varphi_j^k\right)$$

and

$$P_{j/2,\delta_j}\varphi := \frac{1}{2\delta_j}\left(\varphi_{j-1}^{k+1} - \varphi_j^{k+1} + \varphi_{j-1}^k - \varphi_j^k\right).$$

Using Taylor series expansions centered about $\tau_{\frac{j}{2}}$ and $t_{\frac{k}{2}}$ it can be shown (see (A.0.1)) that

$$P^{k/2,\Delta t}\varphi - P_{j/2,\delta_j}\varphi = O((\Delta t)^2) + O(\delta_j^2). \tag{4.2.1}$$

Substituting $e_j^k = \alpha_j^k - \varphi_j^k$ into equation (4.1.13) we arrive at

$$\frac{1}{2\Delta t}\left(e_{j-1}^{k+1} + e_j^{k+1} - e_{j-1}^k - e_j^k\right) + P^{k/2,\Delta t}\varphi = \frac{1}{2\delta_j}\left(e_{j-1}^{k+1} - e_j^{k+1} + e_{j-1}^k - e_j^k\right) + P_{j/2,\delta_j}\varphi. \tag{4.2.2}$$

Using $\Delta t = \delta_j = \delta$ and equation (4.2.1), equation (4.2.2) simplifies to

$$e_j^{k+1} = e_{j-1}^k + O(\delta^3).$$

Then

$$|e_j^{k+1}| \leq |e_{j-1}^k| + M_j\delta^3 \leq \|e^k\|_{\max} + M\delta^3, j \geq 1,$$

where $M_j := \max_{\theta\in[\tau_j,\tau_{j-1}]} |\varphi_{\theta\theta\theta}(t_{k+1},\theta)|$ and $M := \max_{\theta\in[-r,0]} |\varphi_{\theta\theta\theta}(t_{k+1},\theta)|$. It is left to estimate e_0^{k+1}. Substituting e_j^k and ε_j^k into equation (4.1.16) we get

$$\sum_{j=1}^{N} \frac{g_j}{\delta_j}(e_{j-1}^{k+1} - e_j^{k+1}) + \sum_{j=1}^{N} \frac{g_j}{\delta_j}(\varphi_{j-1}^{k+1} - \varphi_j^{k+1}) = b_{21}x(t_{k+1}) - b_{21}\varepsilon^{k+1}. \tag{4.2.3}$$

Subtracting (4.1.5) from the equation above we get

$$\sum_{j=1}^{N} \frac{g_j}{\delta_j}(e_{j-1}^{k+1} - e_j^{k+1}) = J - K - b_{21}\varepsilon^{k+1}, \tag{4.2.4}$$

where $J := \int_{-r}^{0} g(\theta)\frac{\partial}{\partial\theta}\varphi(t_{k+1},\theta)d\theta$ and $K := \sum_{j=1}^{N} \frac{g_j}{\delta_j}(\varphi_{j-1}^{k+1} - \varphi_j^{k+1})$. Rewriting the left side of the equation and solving for e_0^{k+1} we have

$$g_1 e_0^{k+1} = \sum_{j=1}^{N} e_j^{k+1}\left(g_j - g_{j+1}\right) + \delta(J-K) - \delta b_{21}\varepsilon^{k+1}, \tag{4.2.5}$$

where $g_{N+1} = 0$. Since $g_j - g_{j+1} > 0, j \geq 1$, and $J - K = O(\delta^{2-p})$ by Lemma 3.3.1 we have

$$\begin{aligned} g_1|e_0^{k+1}| &\leq \sum_{j=1}^{N} |e_j^{k+1}|\left(g_j - g_{j+1}\right) + \delta|J-K| + \delta|b_{21}||\varepsilon^{k+1}| \\ &\leq \max_{j\geq 1}\{|e_j^{k+1}|\}\sum_{j=1}^{N}\left(g_j - g_{j+1}\right) + c_1\delta^{3-p} + \delta|b_{21}||\varepsilon^{k+1}| \\ &\leq \max_{j\geq 1}\{|e_j^{k+1}|\}g_1 + c_1\delta^{3-p} + \delta|b_{21}||\varepsilon^{k+1}| \\ &\leq \|e^k\|_{\max}g_1 + M\delta^3 g_1 + c_1\delta^{3-p} + \delta|b_{21}||\varepsilon^{k+1}|, \end{aligned} \tag{4.2.6}$$

i.e.,

$$|e_0^{k+1}| \leq \|e^k\|_{\max} + c_3\delta^{3-p} + c_2\delta^p|\varepsilon^{k+1}|$$

where $c_2 := (1-p)|b_{21}|$ and some constants c_1, c_3. Thus

$$\|e^{k+1}\|_{\max} \leq \|e^k\|_{\max} + c_3\delta^{3-p} + c_2\delta^p|\varepsilon^{k+1}|. \tag{4.2.7}$$

Consider

$$x(t_{k+1}) = x(t_k) + \delta\dot{x}(t_{k/2}) + \frac{\delta^3}{24}u_k,$$

where $u_k := \frac{d^3}{dt^3}x(t_k') - \frac{d^3}{dt^3}x(t_k'')$, $t_k', t_k'' \in (t_k, t_{k+1})$. For simplicity we will assume $b_{12}(\theta) \equiv 0$ and let $D_{12}\psi := \int_{-r}^0 a_{12}(\theta)\frac{\partial}{\partial\theta}\psi(\theta)d\theta$. In (4.1.4), solving for $\dot{x}(t)$, and substituting it in the above equation we have

$$\begin{aligned} x(t_{k+1}) &= x(t_k) + \delta b_{11}x(t_{k/2}) + \delta b_{12}y_{t_{k/2}}(0) + \delta D_{12}\varphi(t_{k/2}, \cdot) + \delta f^{k/2} + \frac{\delta^3}{24}u_k \\ &= x(t_k) + \delta b_{11}x(t_{k+1}) - \frac{\delta^2}{2}b_{11}\dot{x}(t_{k/2}) + \delta b_{12}y_{t_{k+1}}(0) - \frac{\delta^2}{2}b_{12}\dot{y}_{t_{k/2}}(0) \\ &\qquad +\delta D_{12}\varphi(t_{k/2}, \cdot) + \delta f^{k+1} - \frac{\delta^2}{2}f'^{k+1} + O(\delta^3), \end{aligned} \tag{4.2.8}$$

where we used Taylor approximations for $x(t)$, $y_t(0)$, and $f(t)$. Similarly, solving for x^{k+1} in the discrete equation (4.1.15) we have

$$\begin{aligned} x^{k+1} &= x^k + \delta b_{11}x^{k+1} + \delta b_{12}\alpha_0^{k+1} + \delta\tilde{D} + \delta f^{k+1} \\ &= x^k + \delta b_{11}x^{k+1} + \delta b_{12}\alpha_0^{k+1} + \delta\tilde{P} + \delta\tilde{E} + \delta f^{k+1}, \end{aligned} \tag{4.2.9}$$

where $\tilde{D} := \sum_{j=1}^N \frac{a_{12j}}{2\delta_j}\left(\alpha_{j-1}^{k+1} - \alpha_j^{k+1} + \alpha_{j-1}^k - \alpha_j^k\right)$, $\tilde{P} := \sum_{j=1}^N \frac{a_{12j}}{2\delta_j}\left(\varphi_{j-1}^{k+1} - \varphi_j^{k+1} + \varphi_{j-1}^k - \varphi_j^k\right)$ and $\tilde{E} := \sum_{j=1}^N \frac{a_{12j}}{2\delta_j}\left(e_{j-1}^{k+1} - e_j^{k+1} + e_{j-1}^k - e_j^k\right)$. Subtracting equation (4.2.9) from (4.2.8) we have

$$\begin{aligned} \varepsilon^{k+1} &= \varepsilon^k + \delta b_{11}\varepsilon^{k+1} - \delta b_{12}e_0^{k+1} + \delta(D_{12}\varphi(t_{k/2}, \cdot) - \tilde{P}) - \delta\tilde{E} + O(\delta^2) \\ &= \varepsilon^k + \delta b_{11}\varepsilon^{k+1} - \delta b_{12}e_0^{k+1} - \delta\tilde{E} + O(\delta^2), \end{aligned}$$

since $D_{12}\varphi(t_{k/2}, \cdot) - \tilde{P} = O(\delta)$ by (A.0.2). By (A.0.3) we have that

$$|\tilde{E}| \leq A\|e^{k+1}\|_{\max} + A\|e^k\|_{\max}.$$

Estimating ε^{k+1}, we have

$$|\varepsilon^{k+1}| \leq |\varepsilon^k| + \delta|b_{11}||\varepsilon^{k+1}| + \delta|b_{12}||e_0^{k+1}| + \delta|\tilde{E}| + c_1'\delta^2$$

$$\leq |\varepsilon^k| + \delta|b_{11}||\varepsilon^{k+1}| + \delta|b_{12}|\|e^{k+1}\|_{\max} + \delta A\|e^{k+1}\|_{\max} + \delta A\|e^k\|_{\max} + c_1'\delta^2.$$

That is,

$$|\varepsilon^{k+1}| \leq (1+a\delta)|\varepsilon^k| + \delta c_1'\|e^{k+1}\|_{\max} + \delta c_2'\|e^k\|_{\max} + c_3'\delta^2, \tag{4.2.10}$$

for some constants a, c_1', c_2', and c_3'. Adding equations (4.2.7) and (4.2.10) and rearranging the terms we have

$$(1-c_2\delta^p)|\varepsilon^{k+1}| + (1-c_1'\delta)\|e^{k+1}\|_{\max} \leq (1+a\delta)|\varepsilon^k| + (1+c_2'\delta)\|e^k\|_{\max} + c_4\delta^2,$$

for some constant c_4. Let $d \geq \max\{c_2, c_1'\}$, $d' \geq \max\{a, c_2'\}$, and note $-\delta^p < -\delta$ for $0 < \delta < 1$. Hence

$$(1-d\delta^p)|\varepsilon^{k+1}| + (1-d\delta^p)\|e^{k+1}\|_{\max} \leq (1+d'\delta)|\varepsilon^k| + (1+d'\delta)\|e^k\|_{\max} + c_4\delta^2.$$

Denoting $\xi^k := |\varepsilon^k| + \|e^k\|_{\max}$ we have

$$\xi^{k+1} \leq \frac{1+d'\delta}{1-d\delta^p}\xi^k + \bar{c}\delta^2 \leq (1+d'\delta)(1+d''\delta^p)\xi^k + \bar{c}\delta^2 \leq (1+\bar{d}\delta^p)\xi^k + \bar{c}\delta^2. \tag{4.2.11}$$

for some constants d'', $\bar{d}$, and $\bar{c}$. By Lemma C.0.1 and noting that $\xi^0 = 0$ (by the initial data) we have that

$$\xi^{k+1} \leq (e^{(k+1)\bar{d}\delta^p} - 1)C'\delta^{2-p} = (e^{t_{k+1}(\Delta t)^{-1}\bar{d}\delta^p} - 1)C'\delta^{2-p} \leq (e^{CN^{1-p}} - 1)C'\delta^{2-p}, \tag{4.2.12}$$

where $C' := \bar{c}(\bar{d})^{-1}$ and $C := T\bar{d}r^{p-1}$. Thus,

$$e^{-CN^{1-p}}\xi^{k+1} \leq (e^{CN^{1-p}} - 1)e^{-CN^{1-p}}C'\delta^{2-p}, \tag{4.2.13}$$

and so $e^{-CN^{1-p}}[|\varepsilon^{k+1}| + \|e^{k+1}\|_{\max}] \leq C'\delta^{2-p}$.

□

In the previous two sections we stated an approximation scheme for a certain SNFDE system and we showed convergence of the approximate solutions directly. As in the scalar case, this scheme yielded a finite-dimensional system. In the next section we discuss stabilization for finite-dimensional systems.

4.3 Stabilizing The Finite-Dimensional System

In the previous chapter we saw that the approximation scheme yields a finite-dimensional system and it is the same case here. In this section we give general comments on the stabilizability of the finite-dimensional system.

For a continuous-time ODE system $\mathbf{y}'(t) = \mathbf{A}\mathbf{y}(t)$, the zero solution is asymptotically stable if all eigenvalues of the matrix $\mathbf{A}$ are on the left-hand side of the complex plane (see [27]). The analogous result pertaining to the discrete-time system $\mathbf{x}(k+1) = \mathbf{K}\mathbf{x}(k)$ is that the eigenvalues of the matrix $\mathbf{K}$ lie (strictly) inside the unit circle in the complex plane (see [29]). Consider a general discrete-time system of the form

$$\mathbf{x}(k+1) = \mathbf{K}\mathbf{x}(k) + \mathbf{H}u(k), \tag{4.3.1}$$

$k \geq 0$, where $\mathbf{x}(k)$ and $\mathbf{H}$ are $N \times 1$, $\mathbf{K}$ is $N \times N$, and $u(k)$ is a scalar. By a stabilizing state feedback control we mean the existence of a sequence of scalars $u(k)$ of the form $u(k) = -\mathbf{G}\mathbf{x}(k)$ where $\mathbf{G}$ is a matrix such that the system

$$\mathbf{x}(k+1) = (\mathbf{K} - \mathbf{H}\mathbf{G})\,\mathbf{x}(k) \tag{4.3.2}$$

is asympotically stable. It is known (see [29]) that the existence of a stabilizing feedback control is gauranteed provided that the rank controllability condition

$$\text{rank}\,[\mathbf{H} : \mathbf{K}\mathbf{H} : \mathbf{K}^2\mathbf{H} : \cdots : \mathbf{K}^{N-1}\mathbf{H}] = N \tag{4.3.3}$$

is satisfied. Assume this property holds. The characteristic equation of system (4.3.2) is given by

$$\det[\lambda \mathbf{I} - \mathbf{K} + \mathbf{H}\mathbf{G}] = \lambda^n + \alpha_1 \lambda^{n-1} + \alpha_2 \lambda^{n-2} + \cdots + \alpha_{n-1}\lambda + \alpha_n = 0, \tag{4.3.4}$$

where $\mathbf{I}$ denotes the $N \times N$ identity matrix. Since the roots of this characteristic equation are the eigenvalues of the matrix, it suffices to choose $\mathbf{G}$ such that the coefficients α_i yield a polynomial with roots inside the unit circle. In other words, this is now a pole placement problem. For large N, this can be computationally intensive. Hence, it is important to understand the stability of system (4.1.1)–(4.1.2) prior to discretization. This is a topic for future work.

Consider again a general system (4.3.1) with $\mathbf{H}$, $\mathbf{K}$, and $u(k)$ as before and assume that the rank condition is satisfied. Let $T := M\Delta t$ denote the final time. The optimal control problem for the finite time process $k = 1, 2, \ldots, M$ is stated as follows: find the optimal control sequence $u(0), u(1), \ldots, u(M-1)$ such that the quadratic performance index

$$J = \frac{1}{2}\mathbf{x}^*(M)\mathbf{S}\mathbf{x}(M) + \frac{1}{2}\sum_{k=0}^{M-1} \left(\mathbf{x}^*(k)\mathbf{Q}\mathbf{x}(k) + u^*(k)\mathbf{R}u(k)\right)$$

is minimized subject to

$$\mathbf{x}(k+1) = \mathbf{K}\mathbf{x}(k) + \mathbf{H}u(k).$$

Here, the * notation denotes the conjugate transpose. $\mathbf{Q}$ is a positive definite or positive semidefinite Hermitian matrix (or real symmetric matrix), $\mathbf{R}$ is a positive definite Hermitian matrix (or real symmetric matrix), and $\mathbf{S}$ is a positive definite or positive semidefinite Hermitian matrix (or real symmetric matrix). Typically, the matrices **Q, R** and **S** are chosen to reflect the importance of the state vector, the control vector, and the final state, respectively. Provided that the rank controllability condition (4.3.3) is satisfied, it is known (see [29]) that the optimal control sequence is given in state feedback form by

$$u(k) = -\mathbf{K}(k)\mathbf{x}(k)$$

where

$$\mathbf{K}(k) = \mathbf{R}^{-1}\mathbf{H}^*(\mathbf{K}^*)^{-1}\left[\mathbf{P}(k) - \mathbf{Q}\right]$$

and $\mathbf{P}(k)$ is a $N \times N$ Hermitian matrix (or $N \times N$ real symmetric matrix). Moreover, $\mathbf{P}$(k) can be computed backwards from the following Riccati matrix equation

$$\mathbf{P}(k) = \mathbf{Q} + \mathbf{K}^*\mathbf{P}(k+1)\left[\mathbf{I} + \mathbf{H}\mathbf{R}^{-1}\mathbf{H}^*\mathbf{P}(k+1)\right]^{-1}\mathbf{K}$$

where $\mathbf{P}(M) = \mathbf{S}$. Furthermore, we also have that the minimum value of the performance index is given by $J_{\min} = \frac{1}{2}\mathbf{x}^*(0)\mathbf{P}(0)\mathbf{x}(0)$. The interested reader is referred to [29] for a detailed derivation of these results.

In the next section we apply the approximation scheme to an example. As an application of the approximation scheme we construct a control candidate to stabilize the original system.

4.4 Numerical Example

We now provide a case study implementing the previously discussed approximation scheme. As an application of the scheme we can construct a forcing function to stabilize the original infinite dimensional problem.

Example 4.4.1

Consider the following 2×2 singular neutral system given in [16].

$$\frac{d}{dt}\left(x(t) + \int_{-1}^{0} y(t+s)ds\right) = y(t) + u(t), \tag{4.4.1}$$

$$\frac{d}{dt}\left(\int_{-1}^{0} (-s)^{-1/2} y(t+s)ds\right) = x(t), \tag{4.4.2}$$

with initial data

$$x(0) = 1, \varphi(s) = 0, s \in [-1, 0], \tag{4.4.3}$$

and $u(t)$ is a possible control term. In the case of $u \equiv 0$, the true solution is given by

$$x(t) = \begin{cases} 1 & 0 < t \leq 1 \\ 1 + \frac{4}{3\pi}(t-1)^{3/2} & 1 < t \leq 2 \end{cases}, \tag{4.4.4}$$

and

$$y(t) = \begin{cases} \frac{2}{\pi}t^{1/2} & 0 < t \le 1 \\ \frac{2}{\pi} + \frac{4}{\pi}(t^{1/2}-1) + \frac{1}{2\pi}(t-1)^2 & 1 < t \le 2 \end{cases}. \tag{4.4.5}$$

The associated fully-discrete system, with $\delta_j = \delta = \Delta t$, and $g_j(s) := \int_{\tau_j}^{\tau_{j-1}} (-s)^{-1/2} ds$, is given by

$$\alpha_j^{k+1} = \alpha_{j-1}^k, j = 1, 2, \ldots, N,$$
$$-x_1^{k+1} + \sum_{j=1}^{N} \frac{g_j}{\delta}(\alpha_{j-1}^{k+1} - \alpha_j^{k+1}) = 0,$$

and

$$\frac{1}{\Delta t}x_1^{k+1} - \frac{1}{2}\alpha_0^{k+1} - \frac{1}{2}\alpha_N^{k+1} = \frac{1}{\Delta t}x_1^k - \frac{1}{2}\alpha_0^k + \frac{1}{2}\alpha_N^k + u^{k+1}.$$

To compute the numerical solution we will use the following system of linear equations to determine x^{k+1} and α_j^{k+1}, $j = 0, 1, 2, ..., N$.

$$\mathbf{K}_1\mathbf{y}^{k+1} = \mathbf{K}_2\mathbf{y}^k + \mathbf{v}^{k+1}, \tag{4.4.6}$$

$$\mathbf{K}_1 := \begin{pmatrix} \frac{1}{\Delta t} & -\frac{1}{2} & 0 & \cdots & \cdots & 0 & -\frac{1}{2} \\ 0 & \frac{g_1}{\delta_1} & \left(\frac{g_2}{\delta_2} - \frac{g_1}{\delta_1}\right) & \cdots & \cdots & \left(\frac{g_N}{\delta_N} - \frac{g_{N-1}}{\delta_{N-1}}\right) & -\frac{g_N}{\delta_N} \\ 0 & 0 & 1 & 0 & \cdots & 0 & 0 \\ 0 & 0 & 0 & 1 & \cdots & 0 & 0 \\ \vdots & \vdots & \ddots & \ddots & \ddots & \vdots & \vdots \\ 0 & 0 & 0 & \cdots & 0 & 1 & 0 \\ 0 & 0 & 0 & \cdots & 0 & 0 & 1 \end{pmatrix}, \mathbf{y}^k := \begin{pmatrix} x_1^k \\ \alpha_0^k \\ \alpha_1^k \\ \alpha_2^k \\ \vdots \\ \alpha_{N-1}^k \\ \alpha_N^k \end{pmatrix},$$

$$\mathbf{K}_2 := \begin{pmatrix} \frac{1}{\Delta t} & -\frac{1}{2} & 0 & \cdots & 0 & \frac{1}{2} \\ 0 & 0 & 0 & \cdots & 0 & 0 \\ 1 & 0 & 0 & ... & 0 & 0 \\ 0 & 1 & 0 & ... & 0 & 0 \\ \vdots & \vdots & \ddots & \ddots & 0 & 0 \\ 0 & 0 & ... & 1 & 0 & 0 \\ 0 & 0 & ... & 0 & 1 & 0 \end{pmatrix}, \text{ and } \mathbf{v}^k := \begin{pmatrix} u^{k+1} \\ 0 \\ 0 \\ \vdots \\ 0 \\ 0 \end{pmatrix}.$$

Remark 4.4.1. The matrix $\mathbf{K}_1$ in (4.4.6) is nonsingular for all N considered in this chapter. ■

At time $t = 0$ we have that $x^0 = 1$ and $\alpha_j^0 = 0$ for $j = 1, ..., N$, by the initial data (4.4.3). Hence, the vector $\mathbf{y}^0$ is known. As in the previous chapter, the vector of unknowns at step $(k+1)\Delta t$, $(x^{k+1}, \alpha_0^{k+1}, \alpha_1^{k+1}, ..., \alpha_{N-1}^{k+1}, \alpha_N^{k+1})^T$, will be computed using $(x^k, \alpha_0^k, \alpha_1^k, ..., \alpha_{N-1}^k, \alpha_N^k)^T$ for $k \geq 1$. The true solution $y(k\Delta t)$ is approximated by $\varphi^N(k\Delta t, 0)$ (since $\theta < 0$ introduces a delay) and so the numerical solution is continuously advanced by the α_0^k component in each newly computed vector. Thus, the numerical solution up to time-step $k+1$ is given by the values $x^1, x^2, \ldots, x^{k+1}$ and $\alpha_0^1, \alpha_0^2, ..., \alpha_0^k, \alpha_0^{k+1}$.

The solution to this equation, with $u \equiv 0$, is shown in Figures 4.1–4.2 with $N = 100$. Equation (4.4.6) can be rewritten as $\mathbf{y}^{k+1} = \mathbf{K}y^k + \mathbf{H}u^{k+1}$, where $\mathbf{K} := \mathbf{K}_1^{-1}\mathbf{K}_2$ and $\mathbf{H} := \mathbf{K}_1^{-1}\mathbf{v}$. We can compute that

$$\text{rank}\, [\mathbf{H} : \mathbf{KH} : \mathbf{K}^2\mathbf{H} : \cdots : \mathbf{K}^{101}\mathbf{H}] = 102,$$

i.e., the controllability matrix indicates that the system is stabilizable. To find a quadratic optimal control sequence we will let $\mathbf{S} = \mathbf{Q} = I$ and $R = 1$, where I is the identity matrix. The results are shown in Figures 4.3–4.4.

We can see that the system is not stabilized. Through numerical experiments it was observed that by scaling the vector $\mathbf{H}$ by δ, i.e., replacing $\mathbf{H}$ with $\delta\mathbf{H}$, we achieve better

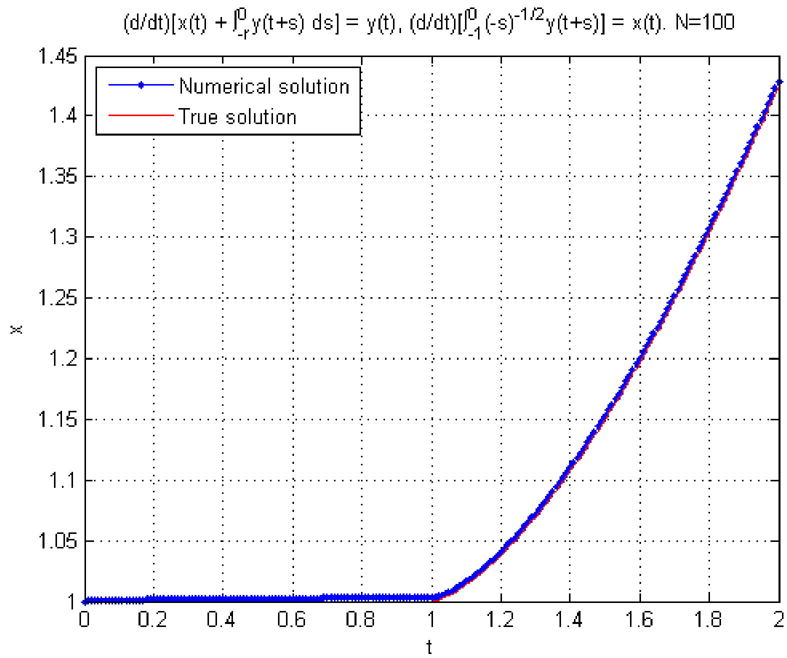

Figure 4.1. Example 4.4.1. True and approximate solution for $x(t)$.

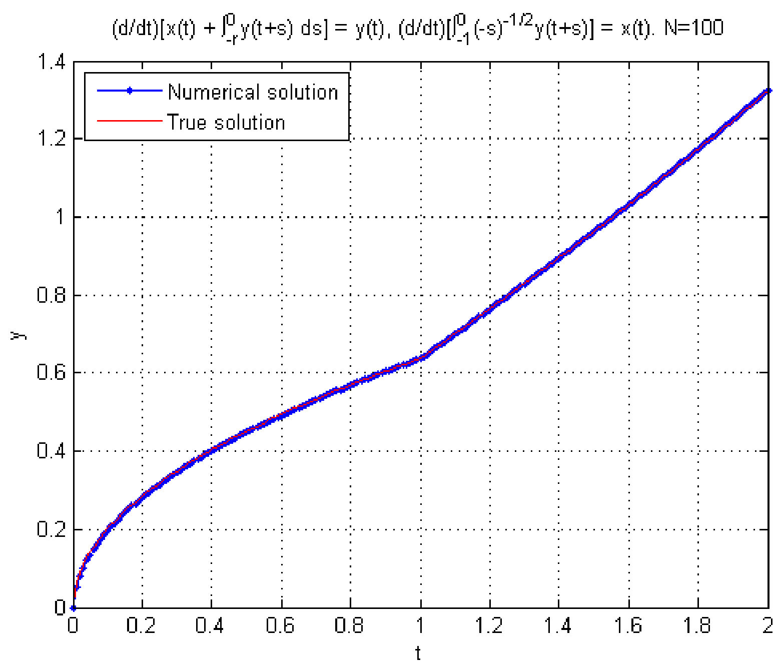

Figure 4.2. Example 4.4.1. True and approximate solutions for $y(t)$.

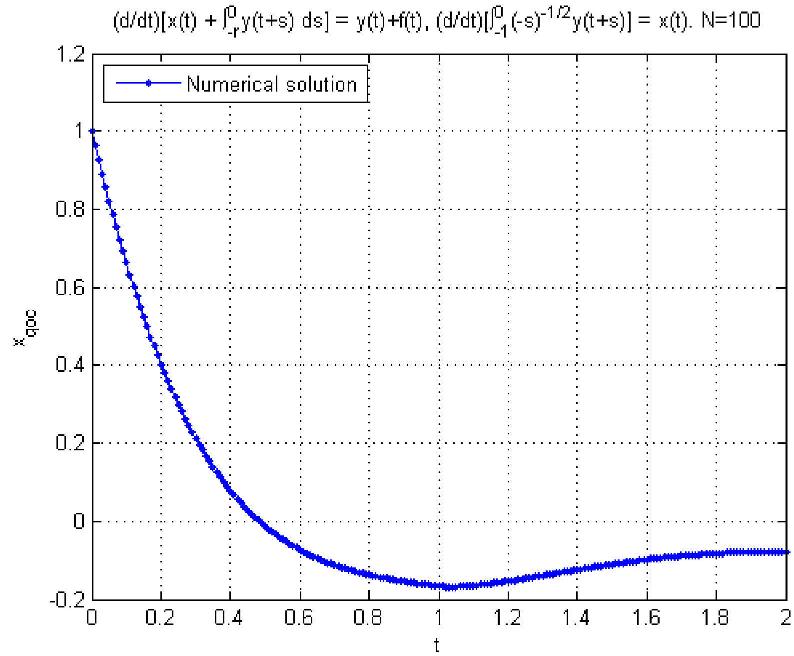

Figure 4.3. Example 4.4.1. Quadratic optimal control for $x(t)$.

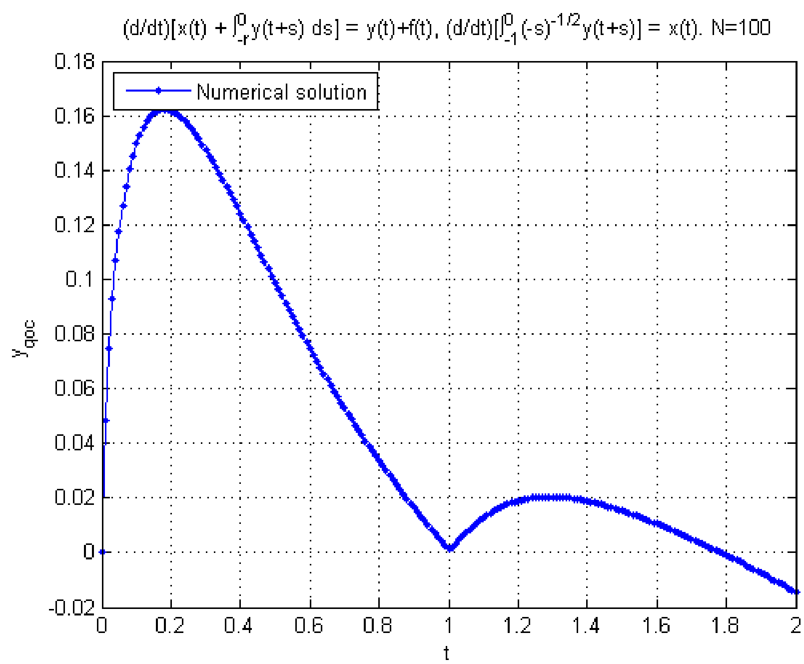

Figure 4.4. Example 4.4.1. Quadratic optimal control for $y(t)$.

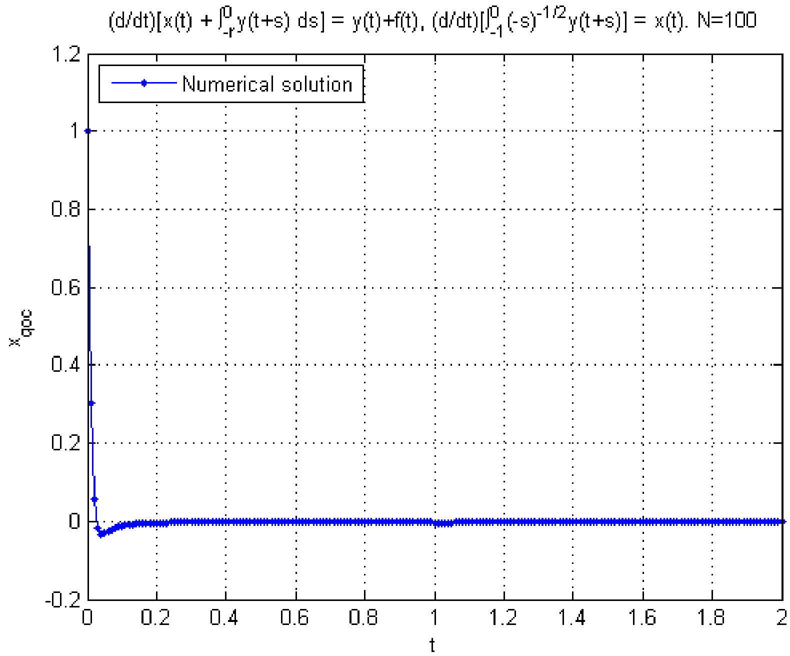

Figure 4.5. Example 4.4.1. Quadratic optimal control for $x(t)$ with scaled $\mathbf{H}$.

numerical results, see Figures 4.5–4.6. It is likely that this resolves numerical errors in the computation in the feedback matrix. In the following section we will discuss numerical considerations.

As an application of the approximation scheme we can construct a finite-dimensional control as a candidate to stabilize the SNFDE (4.4.1)–(4.4.2). Using the sequence of feedback matrices computed for a small mesh size we can construct a control for the original system. More explicitly, for a mesh selection with N subintervals we can compute the control sequence

$$u^k = -\mathbf{K}(k)\mathbf{y}^k$$

for $k = 1, 2, \ldots, T/\Delta t$, where

$$\mathbf{K}(k) = [\eta^k : \beta_0^k : \cdots : \beta_{N+1}^k].$$

Thus

$$u^k = -\eta^k x^k - \beta_0^k \alpha_0^k - \cdots - \beta_{N+1}^k \alpha_{N+1}^k.$$

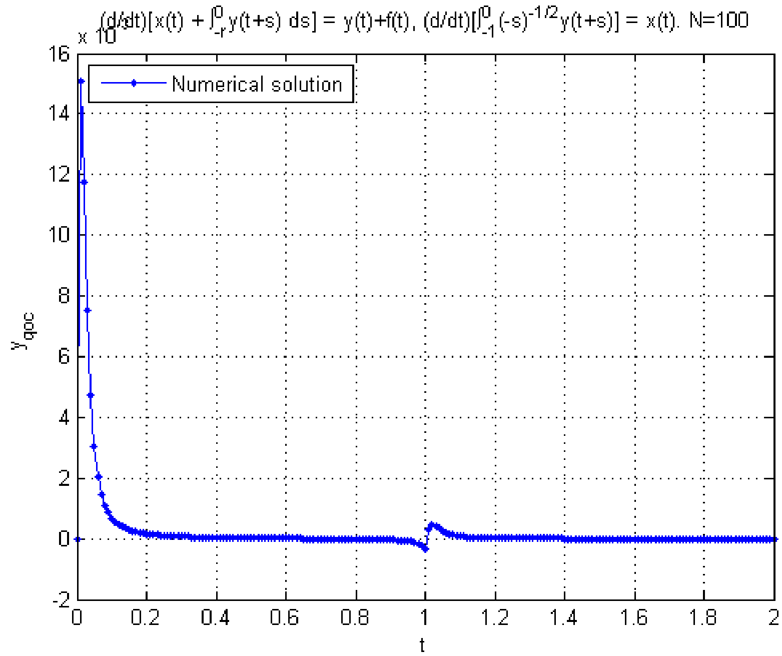

Figure 4.6. Example 4.4.1. Quadratic optimal control for $y(t)$ with scaled $\mathbf{H}$.

This equation indicates the correspondence

$$\eta^k \longmapsto x^k \quad \text{and} \quad \beta_j^k \longmapsto \tau_j^k, j = 0, 1, \ldots, N.$$

Using this correspondence we can construct the forcing function

$$u^k(t) = -\eta^k x(t) - \beta_0^k y_t(0) - \sum_{j=1}^{N} \beta^k y_t(\tau_j), \tag{4.4.7}$$

on the interval $t \in (t_{k-1}, t_k]$. Thus, we will consider this function as a feedback control to bring the state to rest. To test the candidacy of this function we must be able to apply it with a finer mesh. For a larger mesh $\{\tilde{\tau}_j\}_{j=0}^{\tilde{N}}$, where $\tilde{N} \geq N$ and $\{\tau_j\}_{j=0}^{N} \subseteq \{\tilde{\tau}_j\}_{j=0}^{\tilde{N}}$, we can extend (4.4.7) to

$$u^k(t) = -\eta^k x(t) - \beta_0^k y_t(0) - \sum_{j=1}^{\tilde{N}} \tilde{\beta}^k(\tilde{\tau}_j) y_t(\tilde{\tau}_j), \tag{4.4.8}$$

for $t \in (t_{k-1}, t_k]$, where

$$\tilde{\beta}^k(\theta) := \begin{cases} \beta_j^k, & \theta \in [\tau_j^N, \tau_{j-1}^N), \\ 0, & \textit{otherwise} \ . \end{cases} \tag{4.4.9}$$

Thus, the control applied at time $t \in (t_{k-1}, t_k]$ is a weighted sum where the weights, β_j^k, in the delay terms are imposed on the subintervals $[\tau_j, \tau_{j-1})$, respectively. Recalling that we defined $\varphi(t, \theta) = y_t(\theta)$ and substituting the approximating function

$$\varphi^{\tilde{N}}(t, \theta) = \sum_{j=0}^{\tilde{N}} \alpha_j^{\tilde{N}}(t) B_j^{\tilde{N}}(\theta) \text{ for } t \geq 0, -r \leq \theta \leq 0,$$

as defined in (4.1.6), into (4.4.8) yields the approximate control

$$u^k(t) = -\eta^k x(t) - \beta_0^k \alpha_0^{\tilde{N}}(t) - \sum_{j=1}^{\tilde{N}} \tilde{\beta}^k(\tilde{\tau}_j) \alpha_j^{\tilde{N}}(t), \tag{4.4.10}$$

$t \in (t_{k-1}, t_k]$. We can now define the piecewise control

$$U^N(t) := \begin{cases} u^k(t) & t \in (t_{k-1}, t_k], k = 1, 2, \ldots, \\ 0 & \textit{otherwise}, \end{cases} \tag{4.4.11}$$

where we again replace $\mathbf{H}$ with $\delta\mathbf{H}$. We now construct a feedback control using $N = 10$ mesh points. The stabilized solution for $N = 10$ is shown in Figures 4.7–4.8. We want to apply this feedback control to approximations with finer mesh.

In Figures 4.9–4.12 we compute the approximate solutions with $\tilde{N} = 100$ and 1000.

We can see that as the mesh is refined, the state approaches zero. This indicates that a simple control algorithm can be applied to stabilize the SNFDE. More importantly, this indicates that attempts to develope a framework to find an optimal control for the SNFDEs considered in this dissertation will have some benefit.

Remark 4.4.2. In the above example, it was required to test for controllability of the finite-dimensional system via a rank condition. There was no indication that this condition would

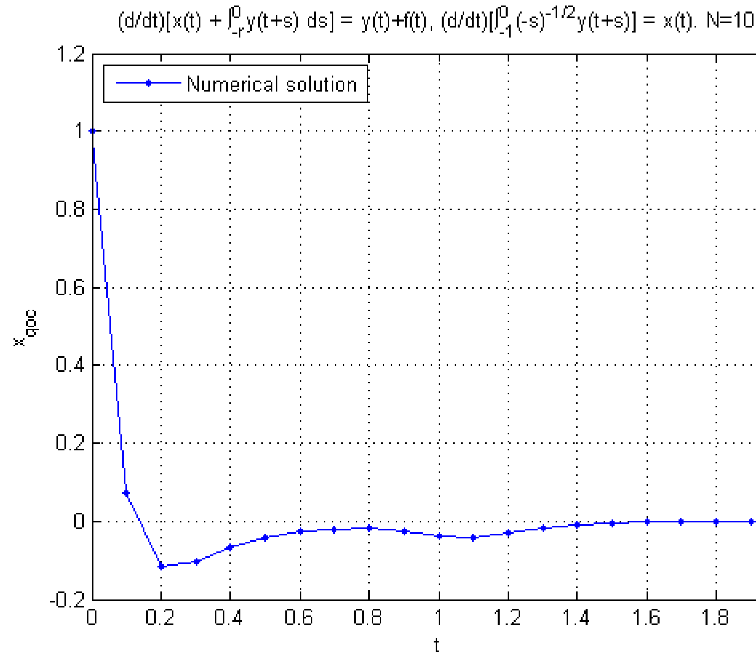

Figure 4.7. Example 4.4.1. Quadratic optimal control for $x(t)$.

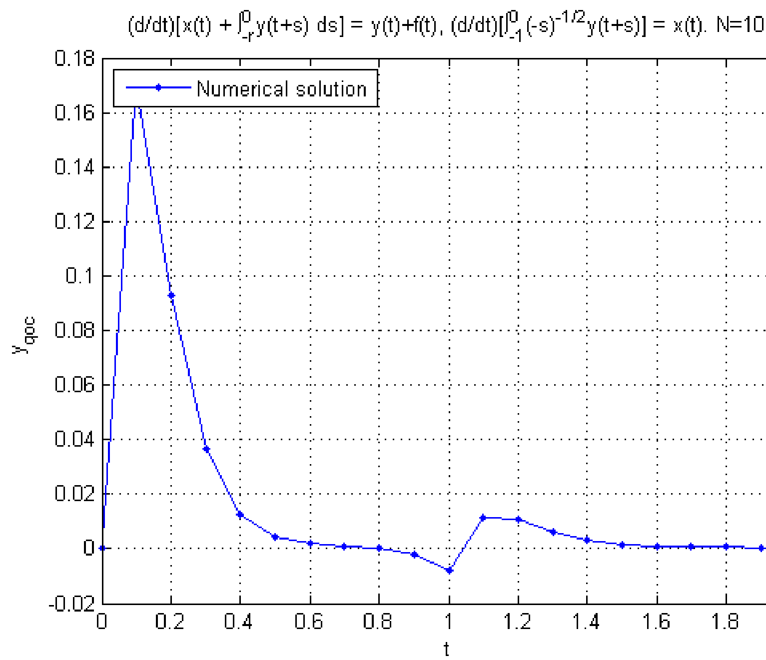

Figure 4.8. Example 4.4.1. Quadratic optimal control for $y(t)$.

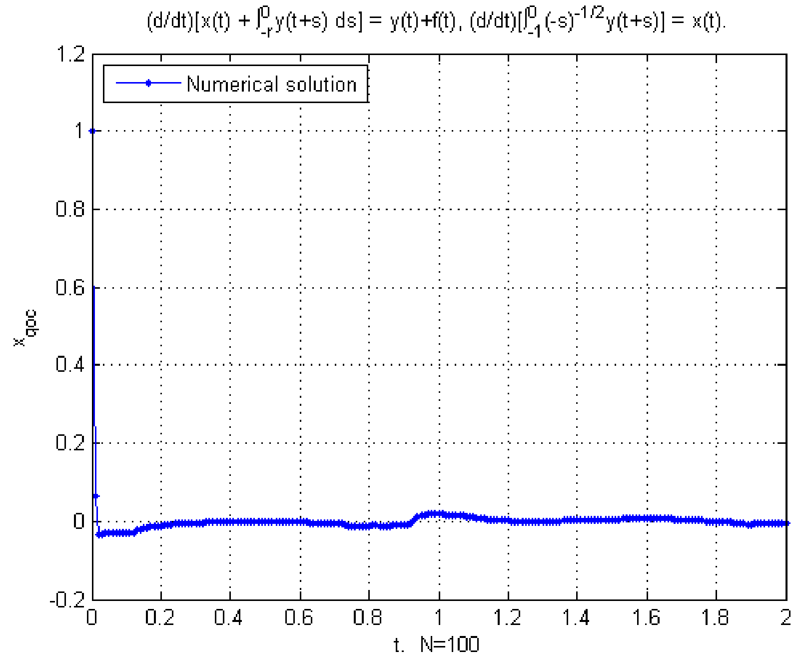

Figure 4.9. Example 4.4.1. Quadratic optimal control for $x(t)$ with control $U^{10}(t)$.

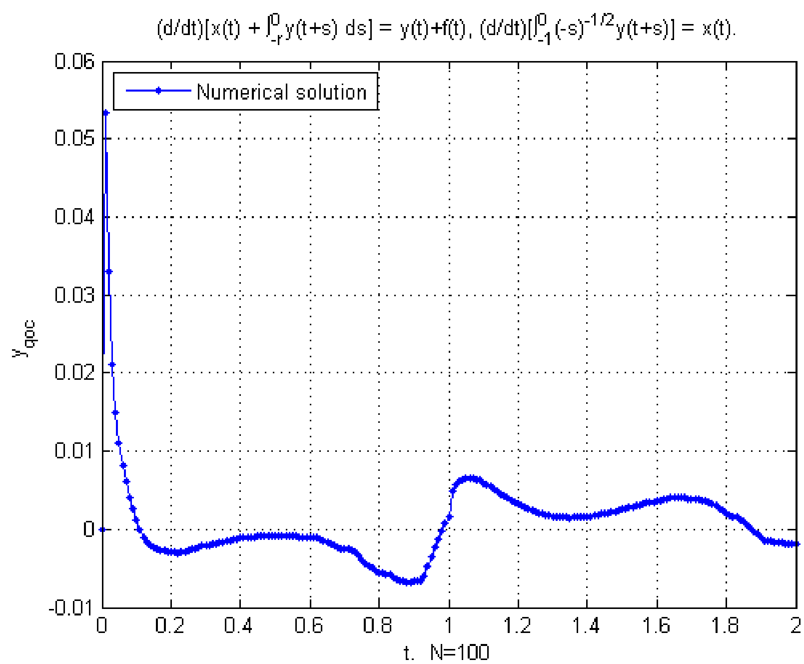

Figure 4.10. Example 4.4.1. Quadratic optimal control for $y(t)$ with control $U^{10}(t)$.

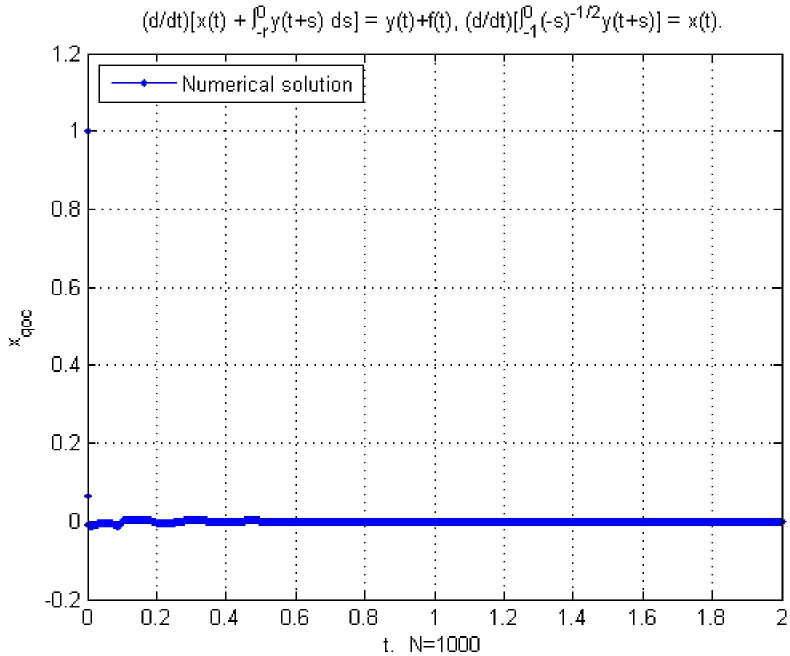

Figure 4.11. Example 4.4.1. Quadratic optimal control for $x(t)$ with control $U^{10}(t)$.

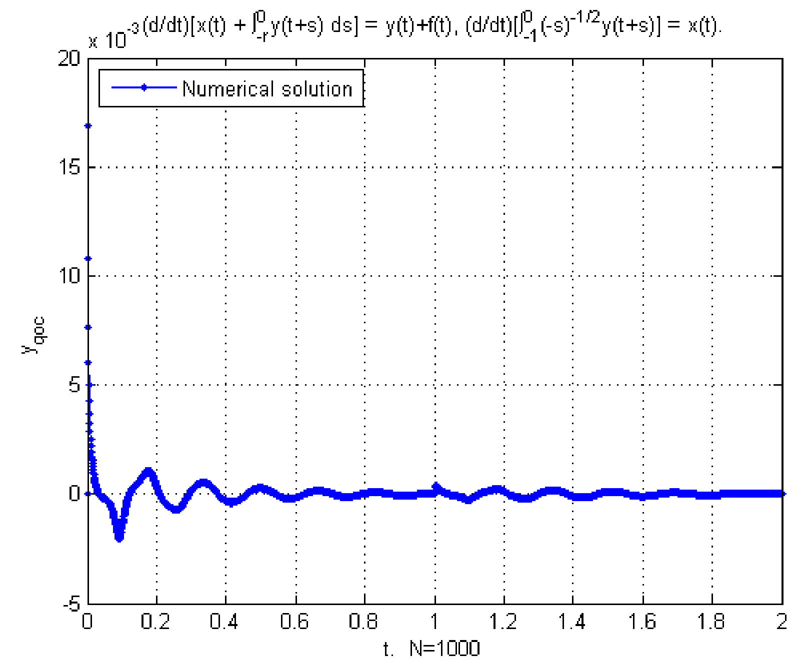

Figure 4.12. Example 4.4.1. Quadratic optimal control for $y(t)$ with control $U^{10}(t)$.

be satisfied prior to discretization. It is unclear if stabilizability of the SNFDE is preserved after discretization. For certain NFDEs, feedback stabilizability is possible provided the difference operator is stable and a rank condition is satisfied (see [13], [14], [28], [30]). See also Appendix B for an overview. To this author's knowledge, similar conditions for SNFDEs are not yet known. ■

4.5 Numerical Considerations

In this section we review some computational issues related to the approximation scheme.

In the previous section we discussed the stabilizability of the finite dimensional system induced by the approximation scheme. In the course of this example we observed numerical difficulties related to the stabilizability. The spectrum of $\mathbf{K}$ is shown in Figure (4.13) for $N = 100$. We can observe that there exists a point in the spectrum near the origin. Additionally, we can compute that the condition number of $\mathbf{K}$ is $\text{cond}(\mathbf{K}) \approx 5.4805$ E+03 for $N = 100$. These observations are troubling since they indicate that $\mathbf{K}$ is nearly singular and that computing its inverse may yield numerical errors. This seems to be the case in the numerical Example 4.4.1 in Figures 4.3–4.4.

4.6 Conclusions

In this section we discussed approximation schemes for an SNFDE system. We presented a lemma establishing convergence of the scheme under certain smoothness conditions. As an application of the approximation scheme we found a control sequence for the associated finite-dimensional system. From this control sequence we constructed a candidate function to stabilize the SNFDE. This forcing function also stabilized the finite-dimensional system as the dimension size is increased. These computations demonstrate that this candidate function may also stabilize the SNFDE. Thus, it is worthwhile to search for results on the

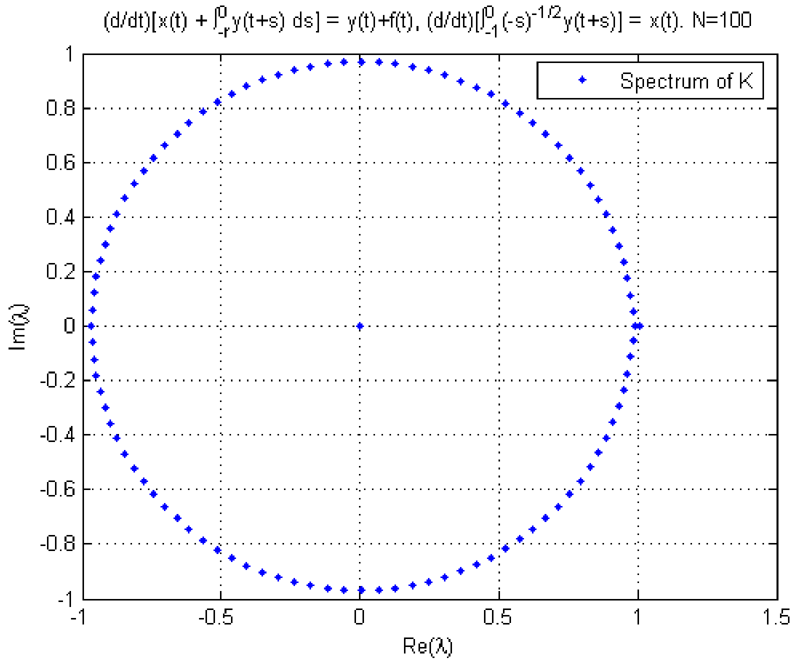

Figure 4.13. Example 4.4.1. Spectrum of **K**.

existence of an optimal control for SNFDEs analogous to the NFDE and RFDE case. This is a topic for future work.

We now give sample Matlab code used in the computations.

4.7 Matlab Code

Sample code for Example (4.4.6).

```
ft=2 ;
N = 10 ; % used to precompute feedback matrix
r=1 ;
dt = r/N ;
T=round(ft/dt) ;
p=0.5 ;
```

```
q = 2 ; % size of system is N^q, after precomputing feedback
    matrix

% approximation scheme
xr=-r ; x0=0 ; x=zeros(1,N+1); x(1) = x0 ;
for n=2:N+1
      x(n) = x(n-1)+(r/N) ;  % uniform
end
x_mesh=-fliplr(x) ; gj=zeros(1,N) ; dj=zeros(1,N);
syms u
for m=1:N
     g = abs(u)^(-p) ;
     gj(m) = int( g, u, x_mesh(m), x_mesh(m+1) ) ;
     dj(m)= abs( x_mesh(m+1) - x_mesh(m) );
end
y_0 = 1 ; phi = x*0 ; %initial conditions
K1=zeros(N+2,N+2) ;  K2=zeros(N+2,N+2) ;  %compute matrices
for j=3:N+2
     Aj=1+dt/dj(N+2-j+1) ; Bj=1-dt/dj(N+2-j+1) ; Cj=Bj/Aj ;
     K1(j,j-1) = Cj ; K1(j,j ) = 1 ;
     K2(j,j-1) = 1 ; K2(j,j) = Cj ;
end
for j=2:N
     K1(2,j+1) = gj(N+1-j)/dj(N+1-j) - gj(N+1-j+1)/dj(N+1-j+1) ;
```

```
end
K1(1,1) = 1/dt ; K1(1,2)= -1/2 ; K1(1,N+2) = -1/2 ;
K1(2,1) = -1 ;
K1(2,2) = gj(N)/dj(N) ; K1(2,N+2) = -gj(1)/dj(1) ;
K2(1,1) = 1/dt ; K2(1,2) = -1/2 ; K2(1,N+2) = 1/2 ; K2(2,1)=1;
% compute QOC
K = K1\K2 ;
S = eye(N+2) ;
Q = eye(N+2) ;
R = 1 ;
v=zeros(N+2,1) ; v(1) = 1 ;
H = dt*K1\v ;
I = eye(N+2) ;
G = zeros( T, N+2 ) ;
P = S ;
cont_matrix = zeros(N+2, N+2);
for k=1:N+2
    cont_matrix(:,k) = K^(k-1)*H ;
end
rank_cond = rank(cont_matrix)
for k=1:T %precompute G matrix for QOC
     P1 = H*(R\H')*P ;
     P2 = (I+P1)\K ;
     P = Q + K'*P*P2 ;
     G1 = R\H' ;
```

```
        G2 = K'\(P-Q) ;
        G( T-k+1,: ) = G1*G2 ;
end

T_1 = T ;
N_1 = N ;

N = N^q ;  % size of new larger system
dt = r/N ;
T=round(ft/dt) ;
p=0.5 ;

G_big = zeros(T, N+2) ; % construct feedback matrix for new larger
    system

T_2 = N_1^(q-1) ;

for m=1:2
for i=1:T_1
        G_big( 1 + T_2*(i-1) : T_2*i , m) = G(i,m) ;
end
end

for j=1:T_1
for m=1:N_1
```

```
        G_big( 1+ T_2*(j-1): T_2*j , 3+ N_1*(m-1): 2 + N_1*(m) ) = G(j,2+m) ;
end
end

% approximation scheme
xr=-r ; x0=0 ; x=zeros(1,N+1); x(1) = x0 ;
for n=2:N+1
        x(n) = x(n-1)+(r/N) ;   % uniform
end
x_mesh=-fliplr(x) ; gj=zeros(1,N) ; dj=zeros(1,N);
syms u
for m=1:N
        g = abs(u)^(-p) ;
        gj(m) = int( g, u, x_mesh(m), x_mesh(m+1) ) ;
        dj(m)= abs( x_mesh(m+1) - x_mesh(m) );
end
y_0 = 1 ; phi = x*0 ; %initial conditions
K1=zeros(N+2,N+2) ;  K2=zeros(N+2,N+2) ;  %compute matrices
for j=3:N+2
        Aj=1+dt/dj(N+2-j+1) ; Bj=1-dt/dj(N+2-j+1) ; Cj=Bj/Aj ;
        K1(j,j-1) = Cj ; K1(j,j ) = 1 ;
        K2(j,j-1) = 1 ; K2(j,j) = Cj ;
end
for j=2:N
```

```
    K1(2,j+1) = gj(N+1-j)/dj(N+1-j) - gj(N+1-j+1)/dj(N+1-j+1) ;
end
K1(1,1) = 1/dt ; K1(1,2)= -1/2 ; K1(1,N+2) = -1/2 ;
K1(2,1) = -1 ;
K1(2,2) = gj(N)/dj(N) ; K1(2,N+2) = -gj(1)/dj(1) ;
K2(1,1) = 1/dt ; K2(1,2) = -1/2 ; K2(1,N+2) = 1/2 ; K2(2,1)=1;
K=K1\K2 ;
v=zeros(N+2,1) ;  v(1) =  1 ;
H = dt*K1\v ;
v_old=[ y_0 , phi]' ;
v_0=v_old ;
y = zeros(T+1,1) ;
a=zeros(T+1,1) ;
y(1) = y_0 ;
a(1)=v_old(2) ;
for k = 1:T ; % compute approximate solution with QOC
    v_new = (K - H*G_big(k,:) )*v_old  ;
    v_old = v_new ;
    y(k+1) = v_old(1) ;
    a(k+1) = v_old(2) ;
end
w = linspace(0,ft,length(a)) ;

figure
plot(w,a,'b.-') ;
```

```
grid on;
title(['(d/dt)[x(t) + \int_{-r}^{0}y(t+s) ds] = y(t)+f(t), (d/dt)
    [\int_{-1}^{0}(-s)^{-1/2}y(t+s)] = x(t).'] ) ;
xlabel(['t.  N=', num2str(N) ]);
ylabel('y_{qoc} ');
legend('Numerical solution','Location','Northwest') ;

figure
plot(w,y,'b.-') ;
grid on;
title(['(d/dt)[x(t) + \int_{-r}^{0}y(t+s) ds] = y(t)+f(t), (d/dt)
    [\int_{-1}^{0}(-s)^{-1/2}y(t+s)] = x(t).'] ) ;
xlabel(['t.  N=', num2str(N) ]);
ylabel('x_{qoc}');
legend('Numerical solution','Location','Northwest') ;
```

CHAPTER 5

CONCLUSIONS AND FUTURE WORK

In this dissertation we discussed approximation schemes for certain classes of SNFDEs.

5.1 Conclusions

In the scalar case we observed that a degredation in the rate of convergence, under uniform mesh, was related to the strength of the weakly singular kernel. This error phenomena was also observed in approximation schemes for Volterra integral equations of second kind. To recover the expected rate we modified the scheme by introducing a graded mesh tailored to the particular SNFDE being considered. This mesh selection strategy was employed in approximation schemes for Volterra equations of second kind and it was observed that it indeed recovers lost convergence rates for such equations. In the case of certain scalar SNFDEs, we presented a lemma and various numerical examples that indicate the graded mesh restores the expected rate of convergence and therefore is a viable alternative to the uniform mesh.

We also considered an approximation scheme for an SNFDE system composed of a neutral equation coupled with a singular neutral equation. We recall that equations of this type occur in certain aeroelastic systems. We established directly the convergence of the scheme under certain smoothness assumptions. As an application of the approximation scheme we constructed a simple feedback stabilizing forcing function using a control sequence for the finite-dimensional system. It was observed that this function also stabilized the numerical solution when the mesh is refined. This indicated that the function also stabilizes the SNFDE. The existence of such a function implies that the search for an optimal control for SNFDEs is a reasonable endevour.

5.2 Future Work

We now give a some brief comments on directions for future work.

In Chapter 3 we provided a suitable modification in the approximation scheme to restore the expected rate of convergence. The results provide a motivation to develope a more complete treatment of the dependence of numerical solutions on mesh selection. In particular, we want to establish attainable optimal rates of convergence for uniform and graded meshes.

In Chapter 4, Remark 4.4.2, we briefly remarked on stabilizability. The theory for the stabilizability of NFDEs is well-developed (see [13], [14], [28], [30]). However, to this authors knowledge, there has not been much development for the case of SNFDEs. In particular, we would like to investigate whether the stability of an SNFDE is preserved after discretization. Without an understanding of the stabilizability of SNFDEs it may be difficult to develop a suitable control framework for such equations. Developing an understanding of stabilizability and optimal control for scalar SNFDEs analogous to NFDEs (see Appendix B) appears to be a reasonable direction for future work.

APPENDIX A

DISCRETIZATION ERRORS

Consistency Error: A

We establish that the discretization for the equation

$$\frac{\partial}{\partial t}\varphi(t,\theta) = \frac{\partial}{\partial s}\varphi(t,s)$$

is second-order in time (t) and second-order in space (s). We first introduce the following discretization operators to simplify notation. Assume $\varphi(t,s)$ is sufficiently differentiable to allow for the Taylor expansions to follow. Let $\varphi_j^k := \varphi(t_k, \tau_j)$ and define

$$P^{k/2,\Delta t}\varphi := \frac{1}{2\Delta t}\left(\varphi_{j-1}^{k+1} - \varphi_{j-1}^{k} + \varphi_j^{k+1} - \varphi_j^k\right)$$

and

$$P_{j/2,\Delta_j}\varphi := \frac{1}{2\Delta_j}\left(\varphi_{j-1}^{k+1} - \varphi_j^{k+1} + \varphi_{j-1}^{k} - \varphi_j^k\right).$$

We first consider the following expansions in space.

$$\varphi((k+1)\Delta t, \tau_{j/2} - \Delta_j/2) = \varphi_j^{k+1} = \varphi_{j/2}^{k+1} - \frac{\Delta_j}{2}\varphi_{s,j/2}^{k+1} + \frac{\Delta_j^2}{2^2\cdot 2}\varphi_{ss,j/2}^{k+1} - \frac{\Delta_j^3}{2^3\cdot 3!}\varphi_{sss}^{k+1}(\xi),$$

$\xi \in (\tau_j, \tau_{j-1})$. Expanding in the other direction we have

$$\varphi_{j-1}^{k+1} = \varphi_{j/2}^{k+1} + \frac{\Delta_j}{2}\varphi_{s,j/2}^{k+1} + \frac{\Delta_j^2}{2^2\cdot 2}\varphi_{ss,j/2}^{k+1} + O(\Delta_j^3).$$

Subtracting these two equations we have

$$\varphi_{j-1}^{k+1} - \varphi_j^{k+1} = \Delta_j\varphi_{s,j/2}^{k+1} + O(\Delta_j^3)$$

In a similar fashion we also have that

$$\varphi_{j-1}^{k} - \varphi_j^{k} = \Delta_j\varphi_{s,j/2}^{k} + O(\Delta_j^3).$$

We now expand in time.

$$\varphi((k+1/2)\Delta t+\Delta t/2,\tau_{j-1})=\varphi_{j-1}^{k+1}=\varphi_{j-1}^{k/2}+\frac{\Delta t}{2}\varphi_{t,j-1}^{k/2}+\frac{(\Delta t)^2}{2^2\cdot 2!}\varphi_{tt,j-1}^{k/2}+\frac{(\Delta t)^3}{2^3\cdot 3!}\varphi_{tt,j-1}(\eta),$$

$\eta\in(k\Delta t,(k+1)\Delta t)$. Likewise, in the other direction we have

$$\varphi((k+1/2)\Delta t-\Delta t/2,\tau_{j-1})=\varphi_{j-1}^{k}=\varphi_{j-1}^{k/2}-\frac{\Delta t}{2}\varphi_{t,j-1}^{k/2}+\frac{(\Delta t)^2}{2^2\cdot 2!}\varphi_{tt,j-1}^{k/2}+O((\Delta t)^3).$$

Subtracting these two previous equations we have

$$\varphi_{j-1}^{k+1}-\varphi_{j-1}^{k}=\Delta t\varphi_{t,j-1}^{k/2}+O((\Delta t)^3).$$

Similarly, we also have

$$\varphi_{j}^{k+1}-\varphi_{j}^{k}=\Delta t\varphi_{t,j}^{k/2}+O((\Delta t)^3).$$

Substituting these terms in the discretization operators we have

$$P^{k/2,\Delta t}\varphi-P_{j/2,\Delta_j}\varphi=\frac{1}{2}\varphi_{t,j-1}^{k/2}+\frac{1}{2}\varphi_{t,j}^{k/2}-\frac{1}{2}\varphi_{s,j/2}^{k+1}-\frac{1}{2}\varphi_{s,j/2}^{k}+O((\Delta t)^2)+O(\Delta_j^2)$$

Note the mixed derivatives exists. Thus we have

$$\varphi_{t,j}^{k/2}=\varphi_{t,j/2}^{k/2}-\frac{\Delta_j}{2}\varphi_{ts,j/2}^{k/2}+O(\Delta_j^2)$$

and

$$\varphi_{t,j-1}^{k/2}=\varphi_{t,j/2}^{k/2}+\frac{\Delta_j}{2}\varphi_{ts,j/2}^{k/2}+O(\Delta_j^2)$$

Adding these equations we have

$$\varphi_{t,j}^{k/2}+\varphi_{t,j-1}^{k/2}=2\varphi_{t,j/2}^{k/2}+O(\Delta_j^2).$$

Likewise, we have

$$\varphi_{s,j/2}^{k+1}=\varphi_{s,j/2}^{k/2}+\frac{\Delta t}{2}\varphi_{st,j/2}^{k/2}+O((\Delta t)^2)$$

and

$$\varphi^k_{s,j/2} = \varphi^{k/2}_{s,j/2} - \frac{\Delta t}{2}\varphi^{k/2}_{st,j/2} + O((\Delta t)^2).$$

Adding these equations we have

$$\varphi^{k+1}_{s,j/2} + \varphi^k_{s,j/2} = 2\varphi^{k/2}_{s,j/2} + O((\Delta t)^2).$$

Thus we have

$$P^{k/2,\Delta t}\varphi - P_{j/2,\Delta_j}\varphi = \varphi^{k/2}_{t,j/2} - \varphi^{k/2}_{s,j/2} + O((\Delta t)^2) + O(\Delta_j^2) = O((\Delta t)^2) + O(\Delta_j^2), \quad \text{(A.0.1)}$$

where $\varphi^{k/2}_{t,j/2} - \varphi^{k/2}_{s,j/2} = 0$ follows from the given equation $\varphi_t(t,s) = \varphi_s(t,s)$. The consistency error is now established.

Consistency Error: B

Let $t_{k+1} := (k+1)\Delta t > 0$ and $\varphi \in C^3([-r,0];\mathbb{R})$. We shall use the notation $\tau_{j/2} := (\tau_{j-1} + \tau_j)/2$ and $\varphi^k_j = \varphi(t_k, \tau_j)$. Define the following discretization operators

$$\tilde{A}_j := \frac{a_{12j}}{2\delta_j}(\varphi^{k+1}_{j-1} - \varphi^{k+1}_j + \varphi^k_{j-1} - \varphi^k_j),$$

$$A_j := \int_{\tau_j}^{\tau_{j-1}} a_{12}(\theta)\varphi_\theta(t_{k/2}, \theta)d\theta,$$

$j = 1, 2, \ldots, N$. Define

$$\tilde{A} := \sum_{j=1}^N \tilde{A}_j \text{ and } A := \sum_{j=1}^N A_j.$$

We want to establish the estimate

$$\tilde{A} - A = O(\delta).$$

Using straightforward calculations involving the Taylor series expansion of $\varphi(t,\theta)$ with respect to its both arguments around $\tau_{\frac{j}{2}}$ and $t_{\frac{k}{2}}$ we obtain the estimate

$$\frac{1}{2\delta_j}\left(\varphi^{k+1}_{j-1} - \varphi^{k+1}_j + \varphi^k_{j-1} - \varphi^k_j\right) = \varphi^{k/2}_{\theta,j/2} + O(\delta_j^2) + O((\Delta t)^2).$$

From this equation we arrive at

$$|\tilde{A}_j - a_{12j}\varphi^{k/2}_{\theta,j/2}| \le |a_{12j}|C_1\delta_j^2 + |a_{12j}|C_2(\Delta t)^2$$

for some constants C_1 and C_2. Note

$$A_j - a_{12j}\varphi^{k/2}_{\theta,j/2} = \int_{t_j}^{t_{j-1}} a_{12}(\theta)(\varphi^{k/2}_{\theta}(\theta) - \varphi^{k/2}_{\theta,j/2})d\theta = \varphi^{k/2}_{\theta\theta,j/2}\int_{t_j}^{t_{j-1}} a_{12}(\theta)(\theta-\tau_{j/2})d\theta$$
$$+\int_{t_j}^{t_{j-1}} a_{12}(\theta)E(\theta)d\theta,$$

where $E(\theta) := \frac{1}{2}\varphi^{k/2}_{\theta\theta\theta}(\theta_j)(\theta-\tau_{j/2})^2$, $\theta_j \in (\tau_j, \tau_{j-1})$. Thus

$$|A_j - a_{12j}\varphi^{k/2}_{\theta,j/2}| \le Ma\delta_j^2 + M'a\delta_j^2,$$

where $\theta_j \in (\tau_j, \tau_{j-1})$, $a := \max_{\theta\in[-r,0]}|a_{12}(\theta)|$, $M := \max_{\theta\in[-r,0]}|\varphi^{k/2}_{\theta\theta}(\theta)|$, and $M' := \max_{\theta\in[-r,0]}|\varphi^{k/2}_{\theta\theta\theta}(\theta)|$. Let $\delta_j = \delta$ for all j. From these estimates we have, with $\delta = \Delta t$,

$$|\tilde{A}_j - A_j| \le |\tilde{A}_j - a_{12j}\varphi^{k/2}_{\theta,j/2}| + |a_{12j}\varphi^{k/2}_{\theta,j/2} - A_j| \le |a_{12j}|C\delta^2 + C'a\delta^2 \le a'C\delta^2 + C'a\delta^2$$

for some constants C and C', where $a' := \int_{-r}^{0}|a_{12}(\theta)|d\theta$. Hence, we have

$$|\tilde{A} - A| \le \sum_{j=1}^{N}|\tilde{A}_j - A_j| = O(\delta). \tag{A.0.2}$$

Consistency Error: C

We can rewrite, with $\delta = \delta_j$ for all j,

$$\tilde{E} := \sum_{j=1}^{N}\frac{a_{12j}}{2\delta_j}\left(e^{k+1}_{j-1} - e^{k+1}_{j} + e^{k}_{j-1} - e^{k}_{j}\right)$$

as

$$\sum_{j=0}^{N}\frac{e^{k+1}_j}{2\delta}(a_{12(j+1)} - a_{12j}) + \sum_{j=0}^{N}\frac{e^{k}_j}{2\delta}(a_{12(j+1)} - a_{12j})$$

with $a_{120} = a_{12(N+1)} = 0$. By the mean value theorem for integrals (see [23])

$$a_{12(j+1)} - a_{12j} = a_{12}(\xi_{j+1})\int_{\tau_{j+1}}^{\tau_j} d\theta - a_{12}(\xi_j)\int_{\tau_{j+1}}^{\tau_j} d\theta = \delta(a_{12}(\xi_{j+1}) - a_{12}(\xi_j))$$

$$= \delta(a_{12}'(\tilde{\xi}_j)\varepsilon_j) + O(\delta\varepsilon_j^2),$$

$j = 1, 2, \ldots, N-1$, for some $\xi_{j+1} \in (\tau_{j+1}, \tau_j)$, $\xi_j \in (\tau_j, \tau_{j-1})$, and $\tilde{\xi}_j \in (\xi_{j+1}, \xi_j)$. Hence,

$$|a_{12(j+1)} - a_{12j}| \leq \delta|a_{12}'(\tilde{\xi}_j)||\varepsilon_j| + C\delta\varepsilon_j^2 \leq 2\delta^2|a_{12}'(\tilde{\xi}_j)| + 2C\delta^3.$$

Similarly,

$$a_{121} = a_{12}(\xi_1)\int_{\tau_1}^{\tau_0} d\theta = a_{12}(\xi_1)\delta \quad \text{and} \quad a_{12N} = a_{12}(\xi_N)\int_{\tau_N}^{\tau_{N-1}} d\theta = a_{12}(\xi_N)\delta$$

for some $\xi_1 \in (\tau_1, \tau_0)$ and $\xi_N \in (\tau_N, \tau_{N-1})$. Thus

$$\begin{aligned} |\tilde{E}| &\leq \sum_{j=0}^{N} \frac{|e_j^{k+1}|}{2\delta}|a_{12(j+1)} - a_{12j}| + \sum_{j=0}^{N} \frac{|e_j^{k}|}{2\delta}|a_{12(j+1)} - a_{12j}| \\ &\leq A\|e^{k+1}\| + A\|e^k\| \end{aligned} \tag{A.0.3}$$

for some constant A such that

$$\sum_{j=0}^{N} \frac{1}{2\delta}|a_{12(j+1)} - a_{12j}| \leq A.$$

APPENDIX B

STABILIZABILITY

The possible control application to the aeroelastic system (2.3.1) motivates an understanding of stabilizability for SNFDEs. In the case of NFDEs with atomic difference operator, the stabilizability is related to the characteristic equation associated with the NFDE.

Consider the following NFDE:

$$\frac{d}{dt}Dx_t = Lx_t + Bu(t) \tag{B.0.1}$$

with initial data $x_0 = \varphi$, $\varphi \in C$, B an $n \times 1$ vector, $u(t)$ is a scalar function defined on $t \geq 0$, and

$$D\varphi := \varphi(0) + \int_{-r}^{0} d\mu(s)\varphi(s) \quad \text{and} \quad L\varphi := \int_{-r}^{0} d\eta(s)\varphi(s).$$

Here, D and L are bounded linear operators where D is atomic at $s = 0$. We are interested in the stability of the zero solution. The zero solution is said to be asymptotically stable if $x(t;\varphi) \longrightarrow 0$ as $t \longrightarrow 0$ for all $\varphi \in C$ in the sup norm. Additionally, we say the NFDE (B.0.1) is stabilizable by state feedback if there is a linear operator $K : C \longrightarrow \mathbb{R}$ such that the closed-loop system

$$\frac{d}{dt}Dx_t = Lx_t + BK(x_t)$$

is an NFDE and the zero solution is asymptotically stable. The possibility of feedback stabilization is related to the stability of the difference operator D. See, for example, [13],[28] and [30]. We discuss this next.

We will say that the operator D is stable if there exists a $\delta > 0$ such that all roots of the equation

$$\det \triangle_D(\lambda) = 0$$

satisfy $\mathrm{Re}\ \lambda \leq -\delta$, where

$$\triangle_D(\lambda) := I_n + \int_{-r}^{0} e^{\lambda s} d\mu(s)$$

and I_n is the $n \times n$ identity matrix. An equation with a stable D operator has the following property (see [13]): if D is stable, then there exists a constant $a_D < 0$ such that for any $a > a_D$, there exist only a finite number of roots λ of the characteristic equation with Re $\lambda > a$. This is important for the following reason: if D is stable and if there exist roots with Re $\lambda > 0$ then there are only a finite number of them. In this case, it is known (see [30]) that feedback stabilization is possible if and only if rank$[\triangle(s)\ B] = n$ for Re $\lambda \geq 0$, where

$$\triangle(\lambda) := \lambda I_n + \lambda \int_{-r}^{0} e^{\lambda s} d\mu(s) - \int_{-r}^{0} e^{\lambda s} d\eta(s).$$

Currently, a comprehensive study of feedback stabilizability for SNFDEs has not yet been developed. A similar stability condition for a non-atomic difference operator would give insight into whether stabilizabity of the SNFDE (2.4.1)–(2.4.3) is possible. A possible first step to understanding the stabilizability of this SNFDE is through numerical experimentation.

APPENDIX C

ANALYSIS

In this section we give a review of preliminary analysis concepts.

Definition C.0.1. A function f definied on an interval $[a, b]$ is said to be of bounded variation if there is a constant $C > 0$ such that

$$\sum_{k=1}^{n} |f(x_k) - f(x_{k-1})| \leq C$$

for every partition

$$a = x_0 < x_1 < \cdots < x_n = b$$

of $[a, b]$ by points of subdivision $x_0, x_1, \ldots, x_n$.

Definition C.0.2. Let f be a function of bounded variation. Then by the total variation of f on $[a, b]$, denoted by $V_{[a,b]}(f)$, is meant the quantity

$$V_{[a,b]}(f) := \sup \sum_{k=1}^{n} |f(x_k) - f(x_{k-1})|,$$

where the least upper bound is taken over all (finite) partitions of the interval $[a, b]$.

Theorem C.0.1. (See [24]) Every continuous linear functional φ on the space $C[a, b]$ can be represented in the form

$$\varphi(f) = \int_a^b f(x) d\mu(x)$$

where μ is a function of bounded variation on $[a, b]$, and moreover

$$\|\varphi\| = \mathrm{Var}_{[a,b]}(\mu).$$

Definition C.0.3. A function f defined on an interval $[a, b]$ is said to be absolutely continuous on $[a, b]$ if, given any $\varepsilon > 0$, there is a $\delta > 0$ such that

$$\sum_{k=1}^{n} |f(b_k) - f(a_k)| < \varepsilon$$

for every finite system of pairwise disjoint subintervals

$$(a_k, b_k) \subset [a, b],$$

$k = 1, 2, \ldots, n$, of total length

$$\sum_{k=1}^{n} (b_k - a_k) < \delta.$$

We provide [24] and [25] as general references for real and functional analysis concepts.

Definition C.0.4. (See [35]) Let $\|\cdot\|_2$ denote the usual Euclidean 2-norm. The zero solution $\mathbf{x}_0 = 0$ is stable if for any $\varepsilon > 0$, there exists a number $\delta = \delta(\varepsilon) > 0$ such that, if $\|\mathbf{x}(0)\|_2 < \delta$, then $\mathbf{x}(k)$ satisfies $\|\mathbf{x}(k)\|_2 < \varepsilon$ for all $k > 0$. The zero solution is asymptotically stable if it is stable and if there exists a $\delta' > 0$ such that if $\|\mathbf{x}(0)\|_2 < \delta'$ then $\|\mathbf{x}(k)\| \longrightarrow 0$ as $k \longrightarrow \infty$.

In practice, it is more desirable for the zero solution to be asymptotically stable.

Definition C.0.5. Let $\xi(\varepsilon)$, $\varepsilon > 0$, be a real valued function. We say that $\xi(\varepsilon) = O(\varepsilon^p)$ if there exists a constant C, independent of ε, such that $|\xi(\varepsilon)| \leq C\varepsilon^p$ as $\varepsilon \longrightarrow 0$.

Lemma C.0.1. If the numbers ξ_i satisfy estimates of the form

$$|\xi_{i+1}| \leq (1 + \delta)|\xi_i| + B, \delta > 0, B \geq 0, i = 0, 1, 2, \ldots,$$

then

$$|\xi_n| \leq e^{n\delta}|\xi_0| + \frac{e^{n\delta} - 1}{\delta} B.$$

Proof. See [34], Section 7.2.2. $\square$

REFERENCES

[1] Banks, H. T., Burns, J. A., *Hereditary control problems: numerical methods based on averaging approximations*, SIAM J. Control and Optimization 16 (1978), 169–208.

[2] Banks, H. T., Kappel, F., *Spline approximations for functional differential equations*, J. Differential Equations, 34 (1979), 496–522.

[3] Brunner H., *Collocation Methods for Volterra Integral and Related Functional Differential Equations,* Cambridge University Press, Cambridge, 2004.

[4] Brunner, H., *The numerical solution of weakly singular Volterra integral equations by collocation on graded meshes.* Math. Comp. 45 (1985), no. 172, 417437.

[5] Burns, J. A., Cliff, E. M., and Herdman, T. L., *A state-space model for an aeroelastic system,* Proc. 22nd IEEE Conf. Decision and Control, San Antonio, TX, 1983, pp. 1174–1177.

[6] Burns, J. A., Herdman, T. L., and Stech, H. W., *Linear functional-differential equations as semigroups on product spaces.* SIAM J. Math. Anal. 14 (1983), no. 1, 98116.

[7] Burns, J. A., and Ito, K., *On well-posedness of integro-differential equations in weighted L^2-spaces*, Tech. Report No. 11-91, Center for Applied Mathematical Sciences, University of Southern California, CA.

[8] Cao, Y., et al. *Singularity Expansion For A Class of Neutral Equations.* J. Integral Equations Applications 19 (2007), no. 1, 13–32.

[9] Cao, Y., Herdman, T., and Xu, Y., *A hybrid collocation method for Volterra integral equations with weakly singular kernels*, SIAM J. Numer. Anal. 41 (2003), 364–381.

[10] Chukwu, E. N., *Stability and time-optimal control of hereditary systems*, Mathematics in Science and Engineering, 188. Academic Press, Inc., Boston, MA, 1992.

[11] Eggermont, P. P. B., *A New Analysis of the Euler-, Midpoint- and Trapezoidal- Discretization Methods for the Numerical Solution of Abel-type Integral Equations*, Medical Image Processing Group Technical Report No. MIPG34. Department of Computer Science, State University of New York at Buffalo, September, 1979.

[12] Gorenflo, R., and Vessella, S., *Abel Integral Equations: Analysis and Applications*, Springer-Verlag, Berlin, 1991.

[13] Hale, J. K. and Martinez-Amores, *Stability in neutral equations*, Nonlinear Analysis, Theory, Methods and App., Vol. 1 No. 2, 161-173.

[14] Hale, J. K. and Lunel, S. M.V., *Introduction to Functional Differential Equations*, Springer-Verlag, New York, 1993.

[15] Herdman, T. L., Turi, J., *A "Natural" State-Space For An Aeroelastic Control System*, J. Integral Equations Applications 7 (1995), no. 4, 413-424.

[16] Herdman, T. L., Turi, J., *Singular Neutral Equations*, Distributed Parameter Control Systems: New Trends and Applications (1991), Vol. 128, 501-511.

[17] Hochstadt, H., *Integral Equations*, Pure and Applied Mathematics, Wiley-Interscience, New York, 1973.

[18] Ito, K., Kappel, F., and Turi, J., *On well-posedness of singular neutral equations in the state space C.* J. Differential Equations 125 (1996), no. 1, 4072.

[19] Ito, K., and Turi, J., *Numerical methods for a class of singular integro-differential equations based on semigroup approximation.* SIAM J. Numer. Anal. 28 (1991), no. 6, 16981722.

[20] Jahanshahi, S., et al., *Solving Abel integral equations of first kind via fractional calculus.* Journal of King Saud University-Science 27.2 (2015): 161-167.

[21] Kappel, F., *Approximation of neutral functional differential equations in the state space* $\mathbb{R}^n \times L^2$, Colloquia Mathematica Societatis Bolyai 30: Qualitative Theory of Differential Equations, Janos Bolyai Math. Soc. and North Holland Publ. Comp., 1979, 463-506.

[22] Kappel, F. and Zhang, K. P., *On neutral functional-differential equations with nonatomic difference operator.* J. Math. Anal. Appl. 113 (1986), no. 2, 311343.

[23] Kincaid, D. and Cheney, W., *Numerical Analysis*, Second Ed., Brooks Cole Publishing, 1996.

[24] Kolmogorov, A. N., Fomin, S. V., *Introduction Real Analysis*, Translated by Silverman, R. A., Dover, New York, 1975.

[25] Kreyszig, E., *Introductory Functional Analysis with Applications*, Wiley, 1989.

[26] Linz, P., *Analytical and Numerical Methods for Volterra Equations*, SIAM, 1985.

[27] Miller, R. K., Michel, A. N., *Ordinary Differential Equations*, Dover Publications, 2007.

[28] O'Conner, D. A. and Tarn, T. J., *On stabilization by state feedback for neutral differential-difference equations*, IEEE Trans. Autom Control (1983), no. 28, 615-618.

[29] Ogata, K., *Discrete-time Control Systems*, Second Ed., Prentice Hall, 1995.

[30] Pandolfi, L, *Stabilization of neutral functional differential equations*, J. Optimization Theory Appl., vol. 20, Oct. 1976, 191-204.

[31] Pazy, A., *Semigroups of Linear Operators and Applications to Partial Differential Equations*, Springer-Verlag, New York, 1983.

[32] Perez-Nagera, P., and Turi, J., *Numerical solutions for a class of singular neutral functional differential equations on graded meshes,* J. Integral Equations Applications, to appear.

[33] Rahman, M.A., Islam, M.S., Alam, M.M., *Numerical Solutions of Volterra Integral Equations Using Laguerre Polynomials.* Journal of Scientific Research, Vol. 4, Number 2 (2012), 357-364.

[34] Stoer, J., Bulirsch, R., *Introduction to Numerical Analysis,* Texts in Applied Mathematics, Springer, 2002.

[35] Swisher, G. M., *Introduction to Linear Systems Analysis,* Matrix Publishers, Inc., 1976.

[36] Torres, L. J., *Approximation of optimal control problems for nonlinear neutral functional differential equations,* Ph. D. Thesis, The University of Texas at Dallas, Richardson, TX, 1993.

[37] Wazwaz, A. M., *Linear and Nonlinear Integral Equations: Methods and Applications*, Springer, 2011.

BIOGRAPHICAL SKETCH

Pedro Perez-Nagera was born on May 12, 1989 in Stuart, Florida and later moved to Columbus, Georgia. He recieved a Bachelor of Science in Mathematics from Columbus State University in 2012. He joined the Mathematical Sciences department at The University of Texas at Dallas in 2012 as a graduate student and he passed his qualifying exams in 2014. He served as a Graduate Teaching Assistant for the Mathematical Sciences department during his time as a graduate student.

CURRICULUM VITAE

EDUCATION

Master of Science: Mathematics, August 2017
University of Texas at Dallas, Richardson, TX
Teaching Assistant Scholarship Fall 2012 – Present

Bachelor of Science: Mathematics, 2007 – 2012
Columbus State University, Columbus, GA
Dean's List Fall 2008 – Spring 2010, Spring 2011

EXPERIENCE

Graduate Teaching Assistant 2012 – Present
University of Texas at Dallas, Richardson, TX

- Develop lesson plans and lead discussions in classes with over 25 students. Grade quizzes, examinations, and record grades. Program mathematical web assignments to be used by future organized courses.

Research Intern June – July 2011
Texas A&M University, College Station, TX

- Participated in a research project on finite-dimensional frame theory.

Peer Instruction Leader Spring & Fall 2011
Columbus State University, Columbus, GA.

- Led open discussions in a problem review session on selected mathematics topics.

PUBLICATION

Numerical solutions for a class of singular neutral functional differential equations on graded meshes, J. Integral Equations Applications, with Janos Turi, to appear.